

LENTES GRAVITACIONALES EN ASTROFÍSICA Y COSMOLOGÍA

SEMANA - 10

PARTE II: LENTES POR GALÁXIAS Y CÚMULOS DE GALÁXIAS

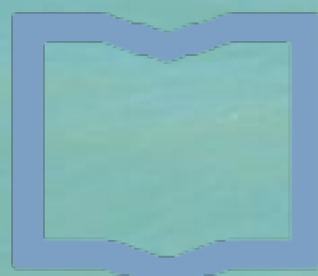
MARTÍN MAKLER

ICAS/IFI/CONICET & UNSAM Y CBPF

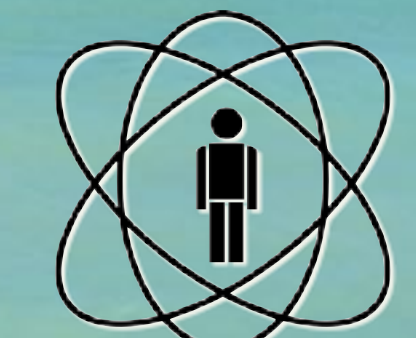
ICAS



CONICET



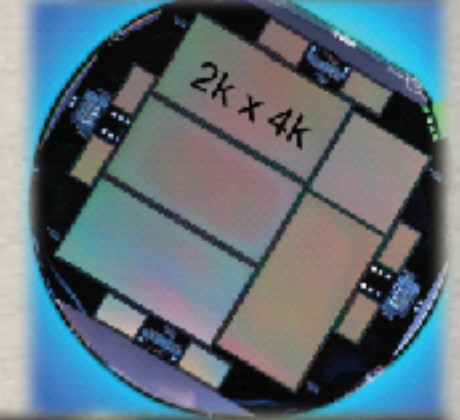
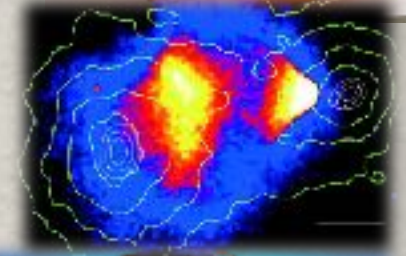
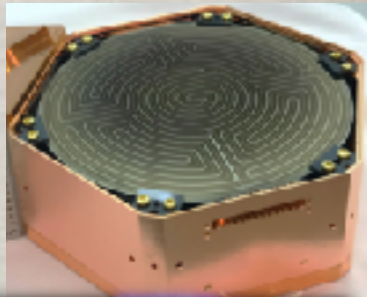
Instituto de
Ciencias Físicas
ICIFI-ECYT_UNSAM-CONICET



CBPF

PLAN DE LA PARTE II

- Redshift y expansión del Universo
- Dinámica y parámetros cosmológicos
- Métrica y distancias
- Energía oscura
- Propagación de la luz y ecuación de la lente
- Lentes extendidas
- Jacobiana de la transformación:
cáusticas y curvas críticas
- Modelos de lentes extendidas y aplicaciones
- Retraso temporal y aplicaciones
- Efecto débil de lentes





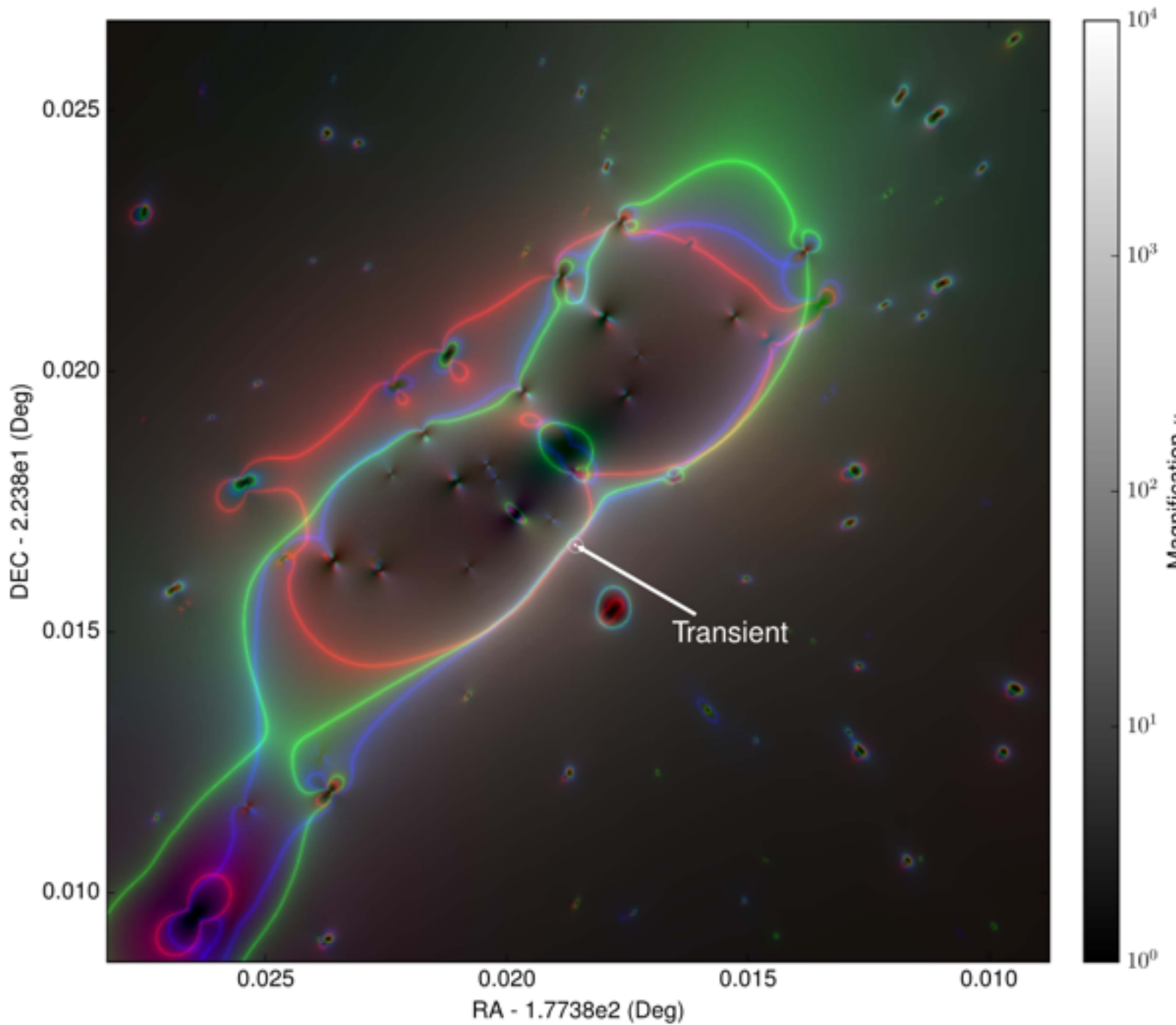
Microlensing of Extremely Magnified Stars near Caustics of Galaxy Clusters

Tejaswi Venumadhav¹ , Liang Dai^{1,4} , and Jordi Miralda-Escudé^{2,3}

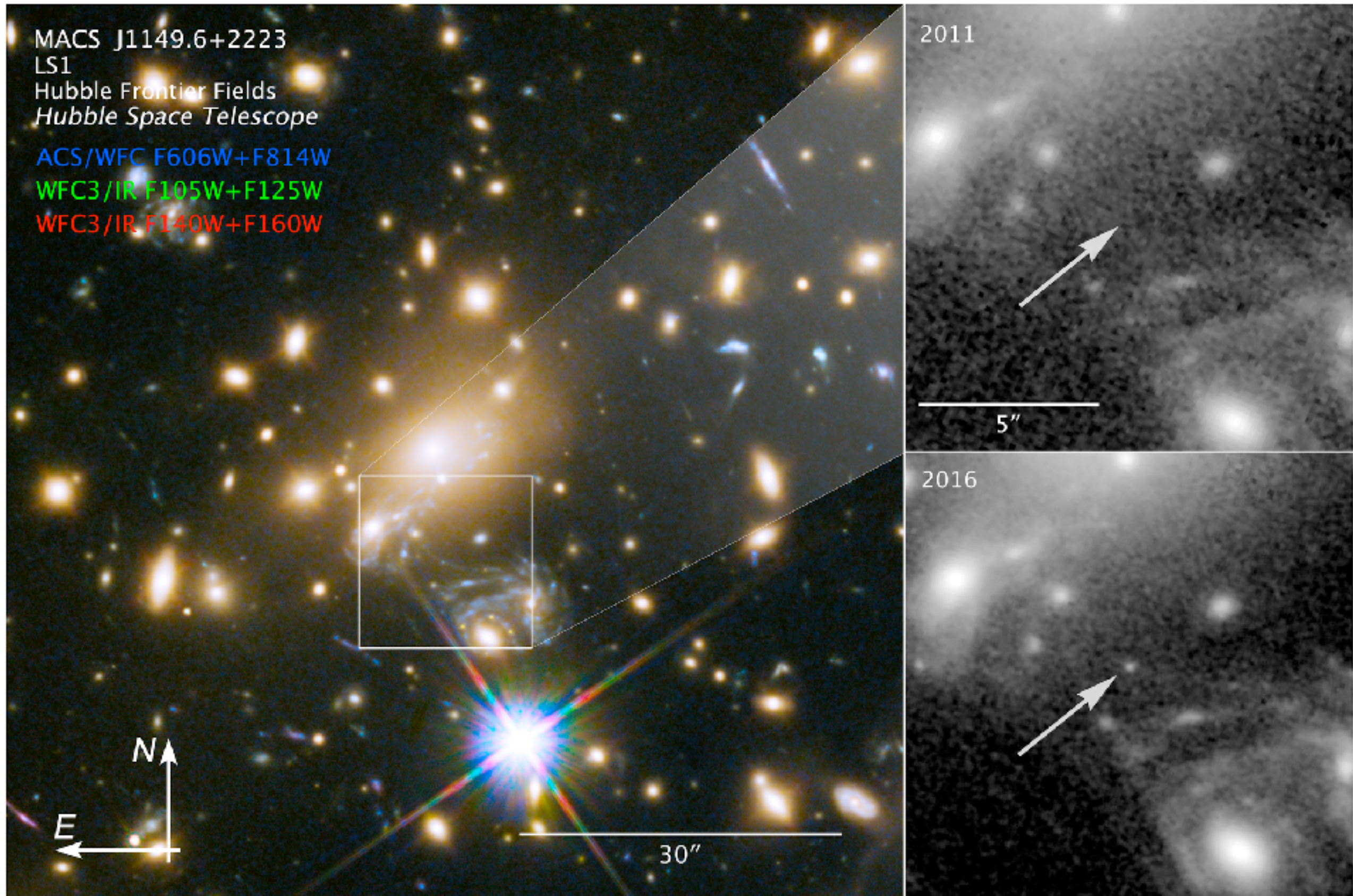
¹ Institute for Advanced Study, 1 Einstein Drive, Princeton, NJ 08540, USA

² Institut Català de Recerca i Estudis Avançats, Barcelona, Catalonia, Spain

³ Institut de Ciències del Cosmos, Universitat de Barcelona IEEC-UB Barcelona E-08028, Catalonia, Spain
Received 2017 June 28; revised 2017 September 30; accepted 2017 October 19; published 2017 November 16



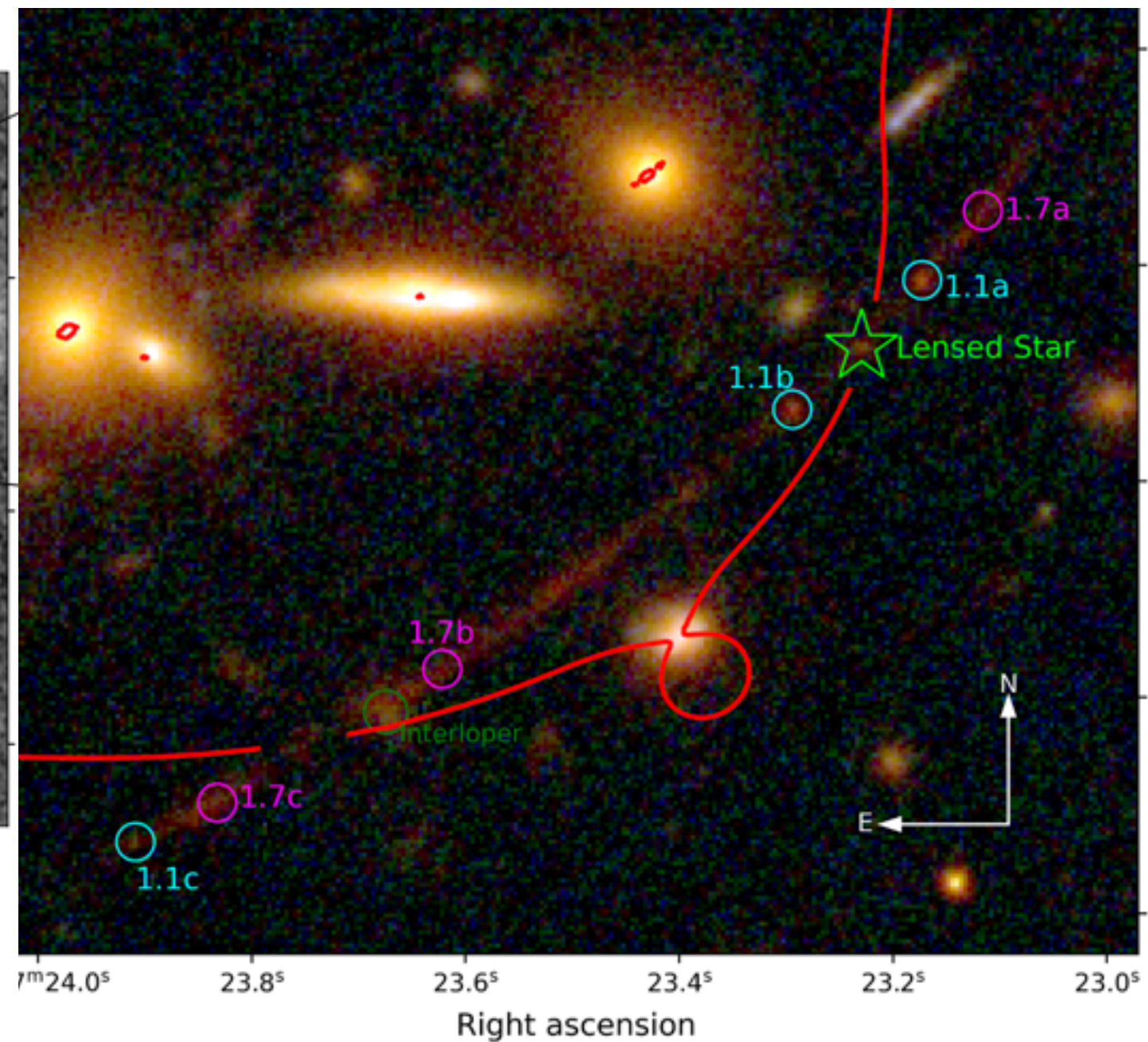
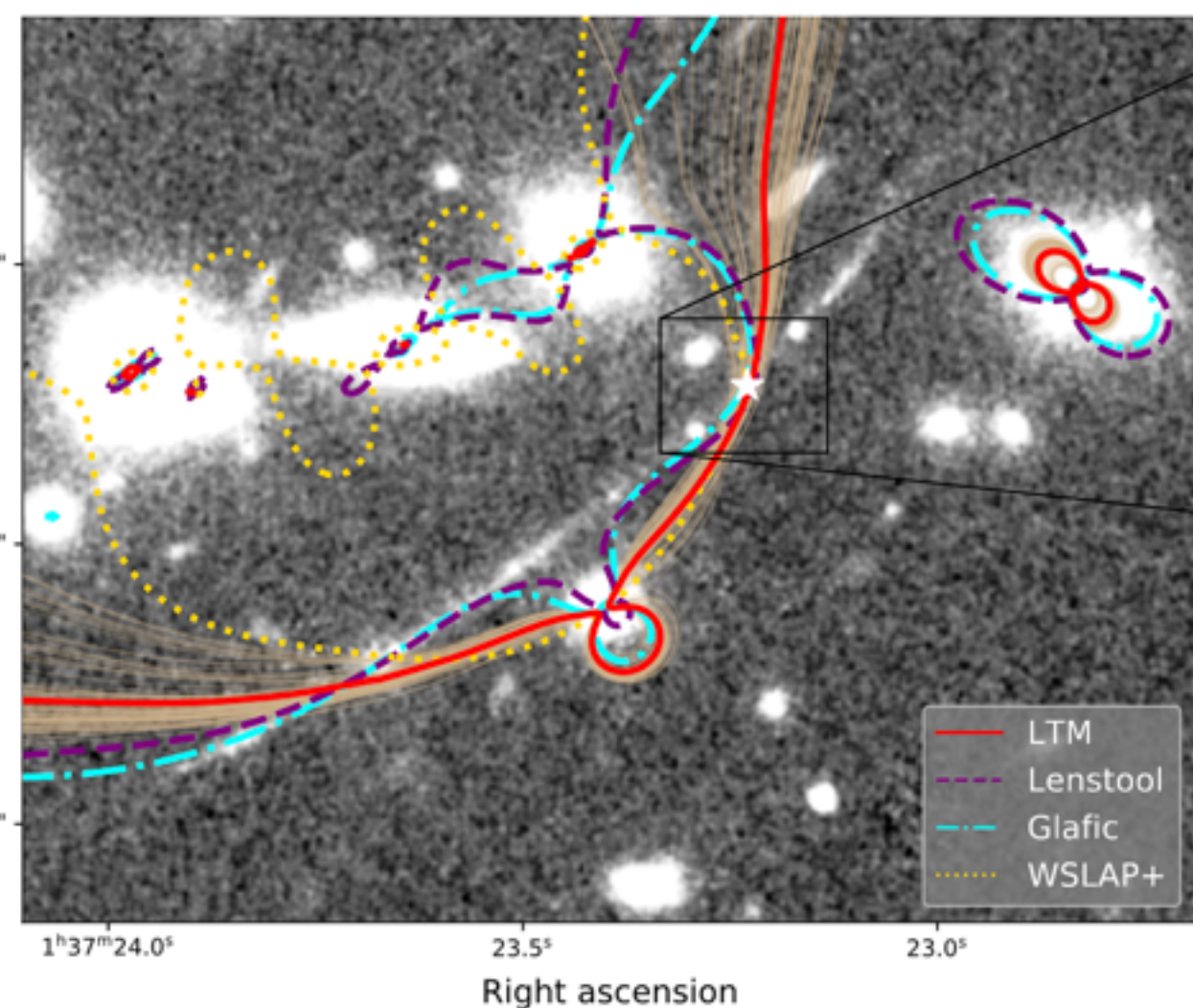
Extreme magnification of an individual star at redshift 1.5 by a galaxy-cluster lens



A highly magnified star at redshift 6.2

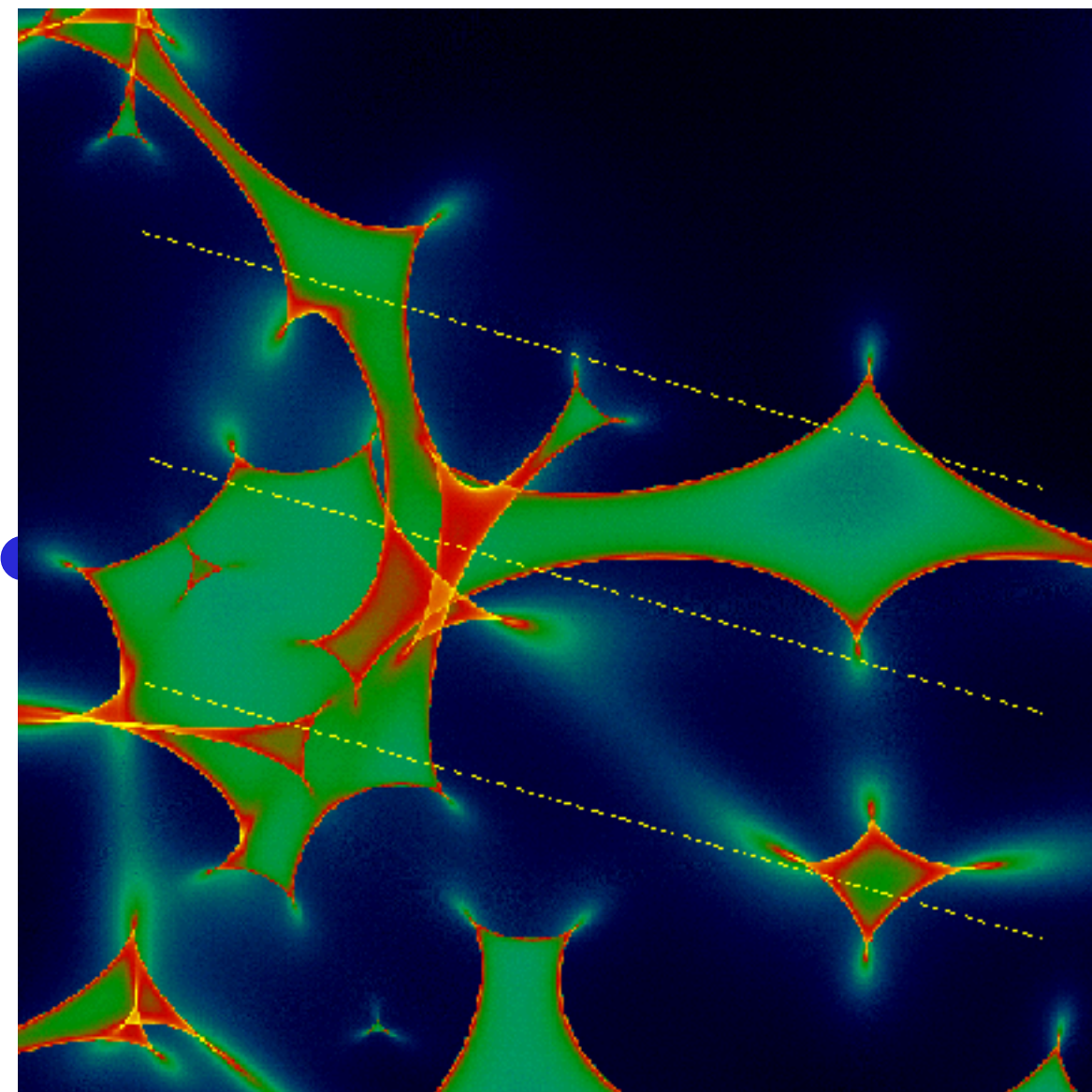
Brian Welch , Dan Coe, Jose M. Diego, Adi Zitrin, Erik Zackrisson, Paola Dimauro, Yolanda Jiménez-Teja, Patrick Kelly, Guillaume Mahler, Masamune Oguri, F. X. Timmes, Rogier Windhorst, Michael Florian, S. E. de Mink, Roberto J. Avila, Jay Anderson, Larry Bradley, Keren Sharon, Anton Vikaeus,

WELCH ET AL.



Mililentes de Cuasares

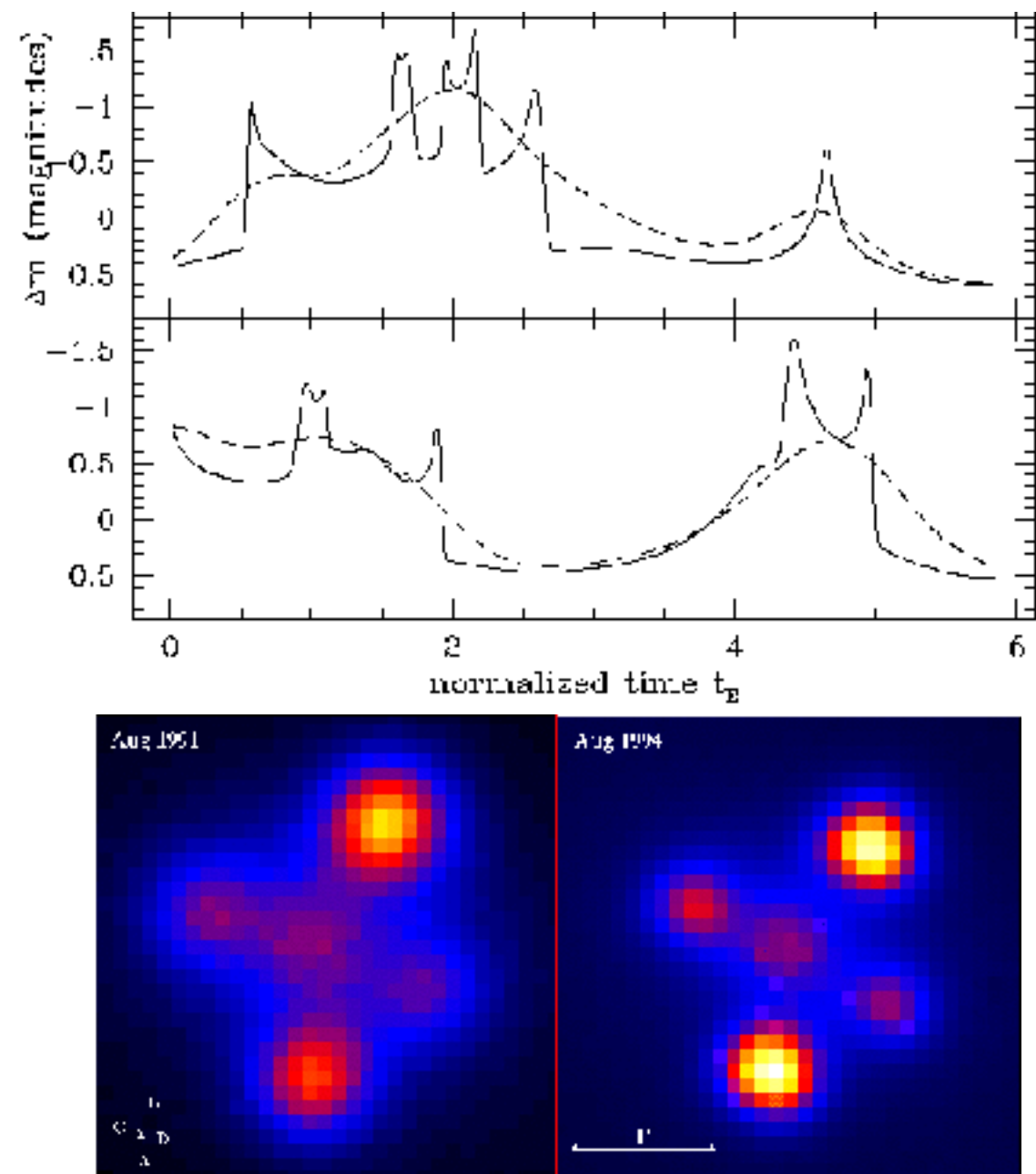
- Patrón de magnificación



Joachim Wambsganss

<http://www.livingreviews.org/lrr-1998-12>

- Curvas de luz



Review actual: arXiv:2312.00931

Probing Extragalactic Planets Using Quasar Microlensing

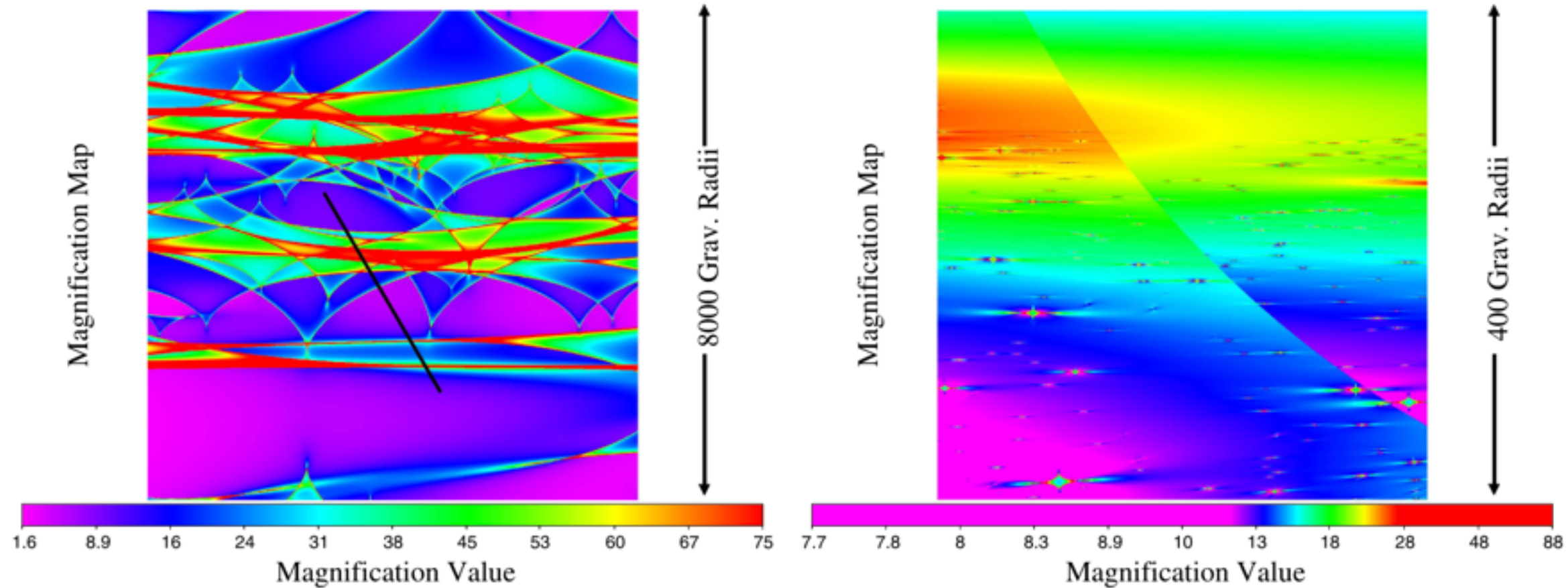
Xinyu Dai  and Eduardo Guerras

Homer L. Dodge Department of Physics and Astronomy, University of Oklahoma, Norman, OK 73019, USA

Received 2017 November 16; revised 2017 December 28; accepted 2018 January 7; published 2018 February 2

Abstract

Previously, planets have been detected only in the Milky Way galaxy. Here, we show that quasar microlensing provides a means to probe extragalactic planets in the lens galaxy, by studying the microlensing properties of emission close to the event horizon of the supermassive black hole of the background quasar, using the current generation telescopes. We show that a population of unbound planets between stars with masses ranging from Moon to Jupiter masses is needed to explain the frequent Fe K α line energy shifts observed in the gravitationally lensed quasar RXJ 1131–1231 at a lens redshift of $z = 0.295$ or 3.8 billion lt-yr away. We constrain the planet mass-fraction to be larger than 0.0001 of the halo mass, which is equivalent to 2000 objects ranging from Moon to Jupiter mass per main-sequence star.



A photograph of a beach scene. The foreground is sandy, with some small debris scattered across it. The middle ground is filled with the turquoise-colored ocean water, showing gentle waves breaking near the shore. The background is a clear, pale blue sky.

TIME DELAYS AND COSMOLOGY

Defasagem temporal gravitacional

Métrica perturbada

$$ds^2 = \left(1 + \frac{2\phi}{c^2}\right) c^2 dt^2 - \left(1 - \frac{2\phi}{c^2}\right) d\sigma^2$$

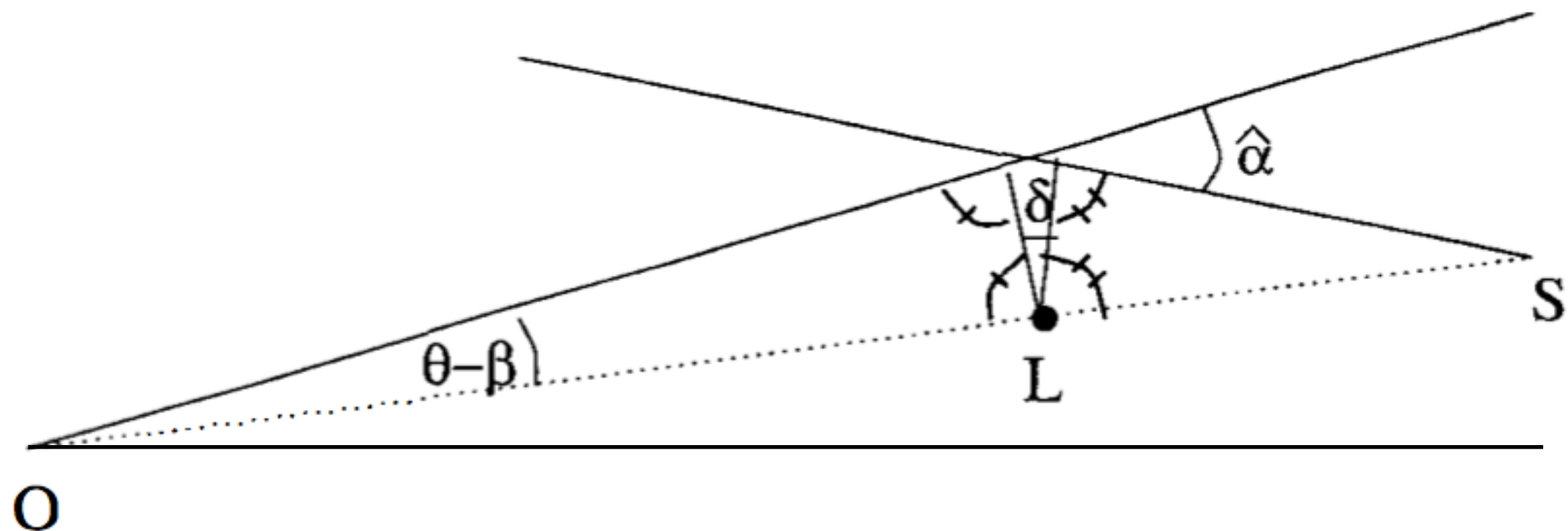
Localmente euclidiano próximo da lente
Geodésica radial

$$t_S - t_0 = \frac{1}{c} \int_{r_O}^{r_S} \left(1 - \frac{2\phi(r)}{c^2}\right) dr$$

Defasagem temporal gravitacional

$$\delta t_{grav} = -\frac{2}{c^3} \int_{r_O}^{r_S} \phi(r) dr = -\frac{2}{c^3} \psi$$

Desvio temporal geométrico



$$\delta L = \frac{D_{OS} D_{OL}}{2 D_{LS}} (\vec{\theta} - \vec{\beta})^2$$

$$\delta t_{\text{geom}} = \delta L / c = \frac{D_{OS} D_{OL}}{2 c D_{LS}} (\vec{\theta} - \vec{\beta})^2$$

Obs.: Dedução rigorosa em Petters, Levine, Wambsganss

Desvio temporal total

Desvio total no referencial da lente

$$\delta t_L = \delta t_{\text{geom}} + \delta t_{\text{grav}}$$

$$\delta t_{\text{geom}} = \delta L/c = \frac{D_{OS}D_{OL}}{2cD_{LS}}(\vec{\theta} - \vec{\beta})^2$$

$$\delta t_{\text{grav}} = -\frac{2}{c^3}\psi \quad \text{mas} \quad \Psi \equiv \frac{2}{c^2} \frac{D_{LS}}{D_{OS}D_{OL}}\psi$$

Assim

$$\delta t_L = \frac{D_{OS}D_{OL}}{cD_{LS}} \left(\frac{1}{2}(\vec{\theta} - \vec{\beta})^2 - \Psi \right)$$

Desvio temporal total

Efeito Doppler

$$\delta t_O / \delta t_L = a_O / a_L = (1 + z_L)$$

$$\delta t_L = \frac{D_{OS} D_{OL}}{c D_{LS}} \left(\frac{1}{2} (\vec{\theta} - \vec{\beta})^2 - \Psi \right)$$

$$\delta t = (1 + z_L) \frac{D_{OS} D_{OL}}{c D_{LS}} \left(\frac{1}{2} (\vec{\theta} - \vec{\beta})^2 - \Psi \right)$$

$\vec{\nabla}_\theta (\delta t) = 0 \rightarrow$ Equação da lente!

Obs.: Dedução rigorosa em Petters, Levine, Wambsganss

Time delay

Geometric + gravitational redshift + Doppler (observer frame)

$$\delta t_L = \delta t_{\text{geom}} + \delta t_{\text{grav}}$$

$$\delta t_{\text{geom}} = \delta L/c = \frac{D_{OS}D_{OL}}{2cD_{LS}}(\vec{\theta} - \vec{\beta})^2 \quad \delta t_{\text{grav}} = -\frac{2}{c^3}\psi$$

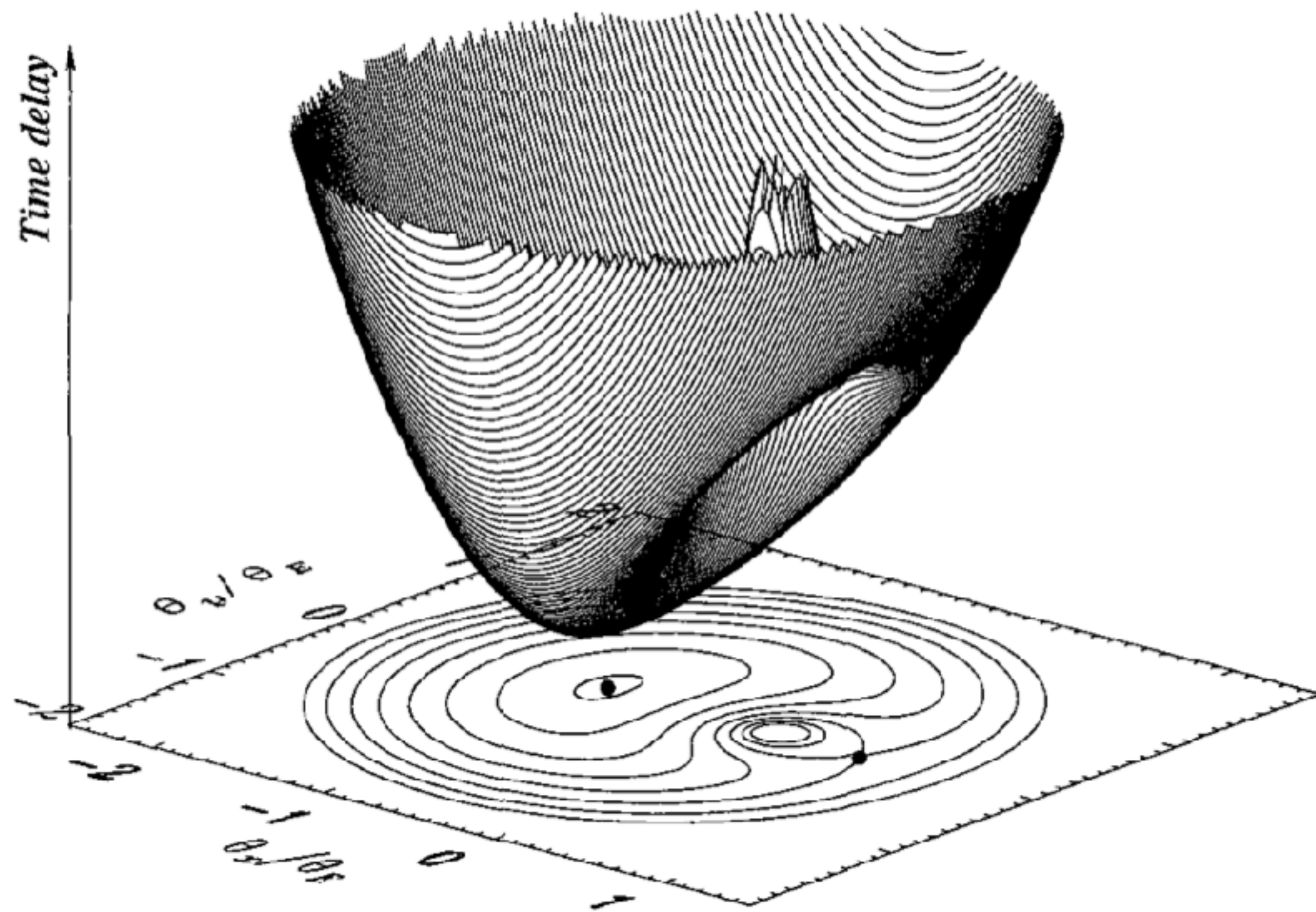
$$\delta t_O / \delta t_L = a_O / a_L = (1 + z_L)$$

$$\Psi \equiv \frac{2}{c^2} \frac{D_{LS}}{D_{OS}D_{OL}} \psi$$

$$\boxed{\delta t = (1 + z_L) \frac{D_{OS}D_{OL}}{cD_{LS}} \left(\frac{1}{2}(\vec{\theta} - \vec{\beta})^2 - \Psi \right)}$$

$$\vec{\nabla}_{\theta}(\delta t) = 0 \rightarrow \text{Lens equation!}$$

Rigorous derivation at Petters, Levine, Wambsganss, sec.(p. 65-76)



Desfasaje temporal y Jacobiana de la transformación

Es fácil ver que

$$\frac{\partial^2 \delta t}{\partial \theta_i \partial \theta_j} \propto \left(\frac{\partial \vec{\beta}}{\partial \vec{\theta}} \right)_{ij} = \delta_{ij} - \frac{\partial^2 \Psi}{\partial \theta_i \partial \theta_j}$$

La curvatura de la función $\delta t(\theta)$ define la paridad de las imágenes

Cuanto menor la curvatura de δt , mayor la magnificación

Segunda derivada se anula \rightarrow magnificación infinita:
Fusión de máximos y puntos de silla (curvas críticas)

Teorema de Burke

Las imágenes se forman a los pares (salvo si hay singularidades) y con distintas paridades)

MULTIPLE GRAVITATIONAL IMAGING BY DISTRIBUTED MASSES¹

WILLIAM L. BURKE

Lick Observatory, Boards of Studies in Astronomy and Astrophysics and in Physics, University of California, Santa Cruz, CA 95064

Received 1980 September 26; accepted 1980 November 5

ABSTRACT

A transparent galaxy, not necessarily spherical, acting as a gravitational lens produces an odd number of images.

Subject headings: galaxies: general — gravitation — quasars

In a recent *Letter* (Dyer and Roeder 1980) it was shown that a transparent spherical galaxy of finite mass acting as a gravitational lens produces an odd number of images. The result is in fact true for arbitrary mass distributions as long as the bending (roughly m/r) remains bounded as r goes to infinity. This covers all realizable cases, since larger masses would be within their own event horizons.

A proof of this stronger result is easy. Parametrize the rays leaving the source by their impact parameters (u, v) , measured in some plane near the deflector and transverse to the rays. See Figure 1. You may think of this plane as the celestial sphere. The action of the gravitational lens bends a ray. Let us look at the intersection of this bent ray with another transverse plane, this one passing through the receiver. We can measure the bending by the direction cosines (s, w) between two lines: one from the source to the point (u, v) in the deflector plane, and one from that point to the point where the actual ray hits the receiver plane. By a transparent deflector we mean one for which all the rays hitting the first plane also hit the second. This excludes solid objects and black holes.

¹ *Lick Observatory Bulletin*, No. 848.

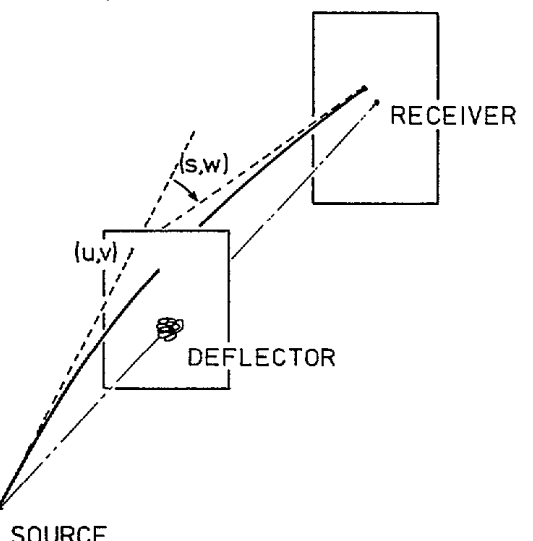


FIG. 1

Dyer, C. C., and Roeder, R. C. 1980, *Ap. J. (Letters)*, 238, L67.

Guillemin, V., and Pollack, A. 1974, *Differential Topology* (Englewood Cliffs, N.J.: Prentice-Hall).

REFERENCES

- Guillemin, V., and Pollack, A. 1974, *Differential Topology* (Englewood Cliffs, N.J.: Prentice-Hall).

The action of the gravitational lens is specified by giving the bendings (s, w) as functions of the impact parameters (u, v) . Such functions can be represented by a vector field on the (u, v) -plane with components (s, w) . A ray with impact parameters (u, v) will reach the receiver only for specific bendings (s, w) . This condition can also be represented as a vector field. The gravitational lens will form an image of the source at the receiver whenever these two vector fields are equal.

Subtract these two vector fields. Our problem is to study the zeros of this difference vector field. Since the bending is assumed bounded, for large impact parameter the difference vector field is dominated by the requirement that it takes a large bend for the ray to reach us. For large impact parameter the difference vector field is mainly radial. The zeros of a vector field on the plane are constrained by the Poincaré-Hopf index theorem (see Guillemin and Pollack 1974), which assigns an index to a region by counting the net rotation of the vector field around the boundary of the region. The index of a region is the sum of the indices around the zeros. Simple zeros of a vector field are either sources, sinks, or saddle points. Sources and sinks have index +1 and correspond to direct images, while saddle points have index -1 and correspond to inverted images (as in Dyer and Roeder's 1980 Fig. 2). The sum of the indices of the zeros for our difference vector field must be +1 because of the behavior at large impact parameter. Thus if there are only simple images, there must be an odd number of them, with one more direct image than inverted images.

Because this is a topological argument the transverse planes need not be flat, the bendings can be measured by angles, tangents, or whatever, and the straight lines need only be straight in some coordinate chart. The (u, v) -plane can be thought of as the celestial sphere of the source or, since rays are reversible, as the celestial sphere of the receiver.

This research was done at the Aspen Center for Physics, and their hospitality and the partial support of the National Science Foundation are gratefully acknowledged.

Time Delay

$$\Delta t_{ij} = \frac{D_\Delta}{c} \left(\frac{1}{2}(\vec{\theta}_i - \vec{\beta})^2 - \Psi(\theta_i) - \frac{1}{2}(\vec{\theta}_j - \vec{\beta})^2 + \Psi(\theta_j) \right)$$

Where $D_\Delta = (1 + z_L) \frac{D_{OS} D_{OL}}{D_{LS}}$

↑

“time delay distance”

inverse modeling
(multiple images)

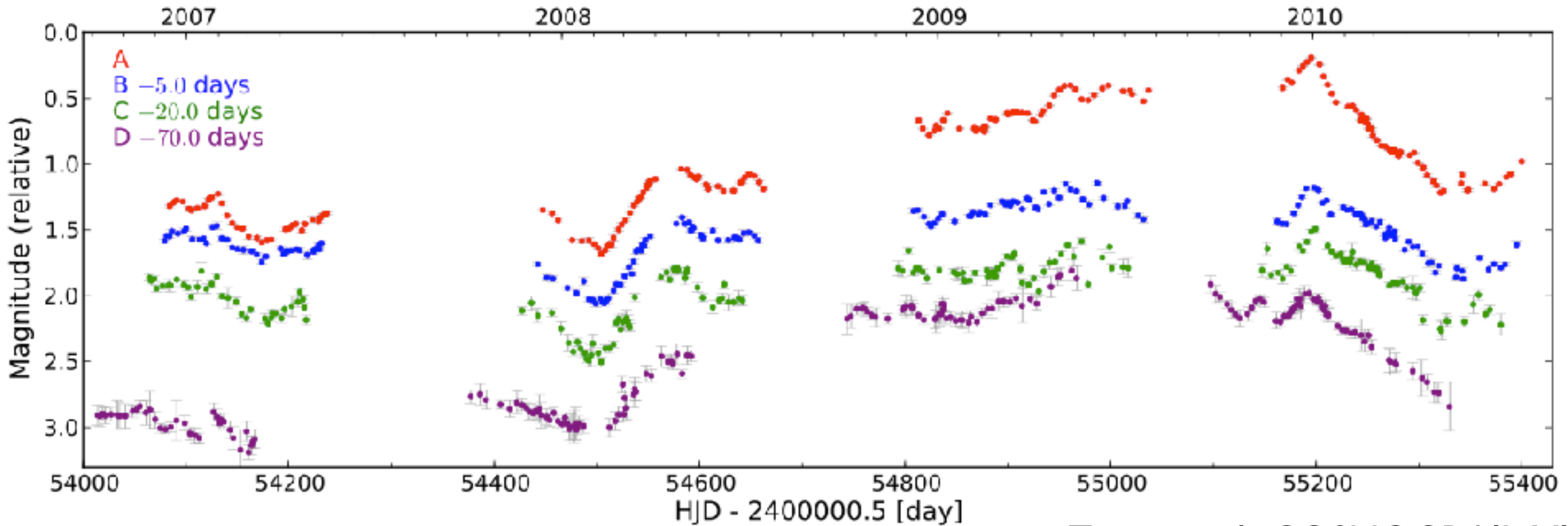
Main cosmological dependence $\propto H_0^{-1}$

Quasar light-curves

Time delay between images

$$\Delta t_{ij} = \delta t(\vec{\theta}_i, \vec{\beta}) - \delta t(\vec{\theta}_j, \vec{\beta})$$

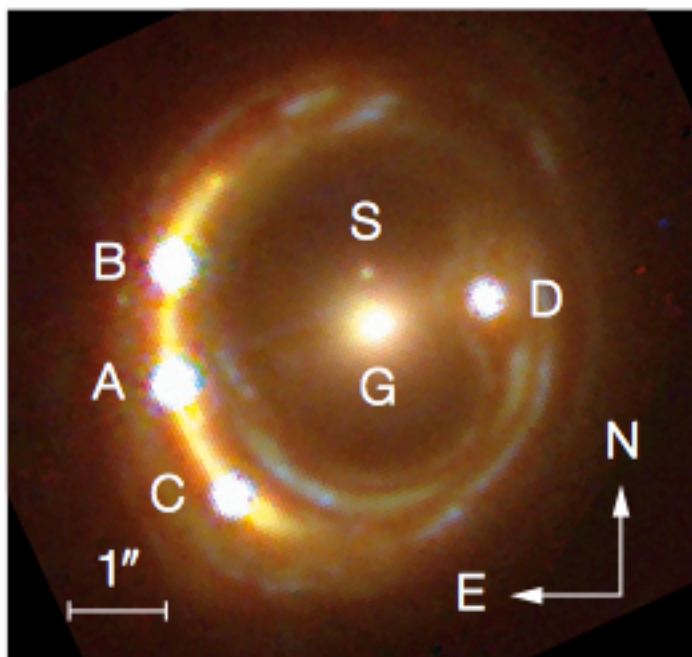
$$= (1 + z_L) \frac{D_{OS} D_{OL}}{c D_{LS}} \left(\frac{1}{2} (\vec{\theta}_i - \vec{\beta})^2 - \Psi(\theta_i) - \frac{1}{2} (\vec{\theta}_j - \vec{\beta})^2 + \Psi(\theta_j) \right)$$



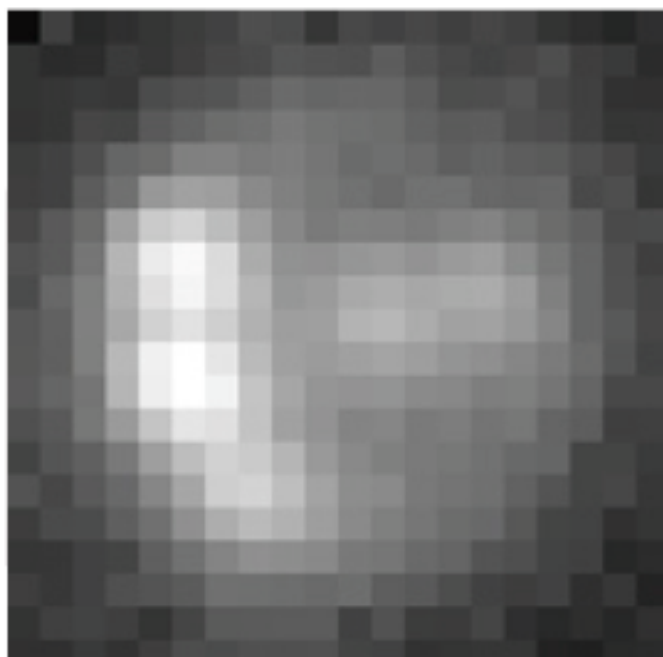
Exemplo: RX J1131-1231

- COSMOGRAIL: the COSmological MOnitoring of GRAvitational Lenses
- Curvas de luz + modelo da lente (+“tudo”)

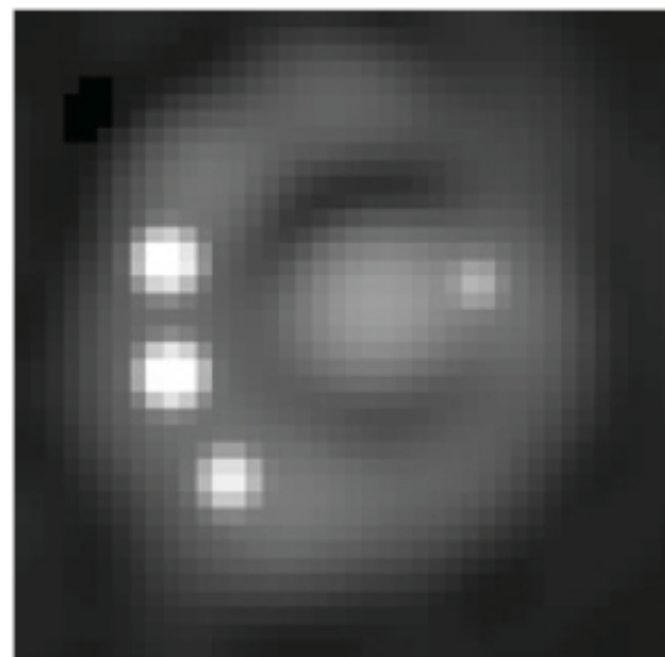
$$\kappa_{\text{pl}}(\theta_1, \theta_2) = \frac{3 - \gamma'}{2} \left(\frac{\theta_E}{\sqrt{q\theta_1^2 + \theta_2^2/q}} \right)^{\gamma' - 1}$$



Hubble Space Telescope

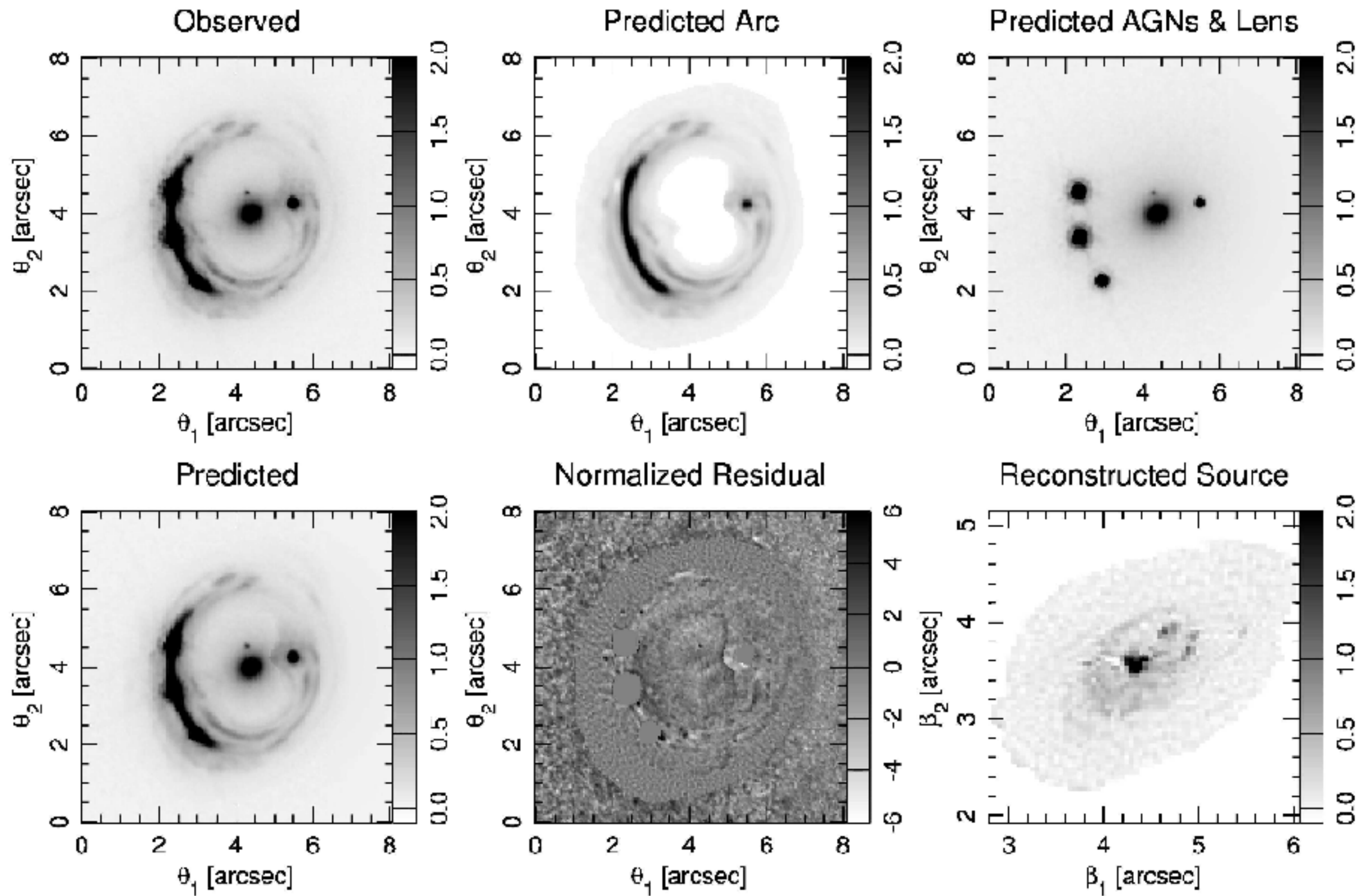


Swiss Leonhard Euler Telescope

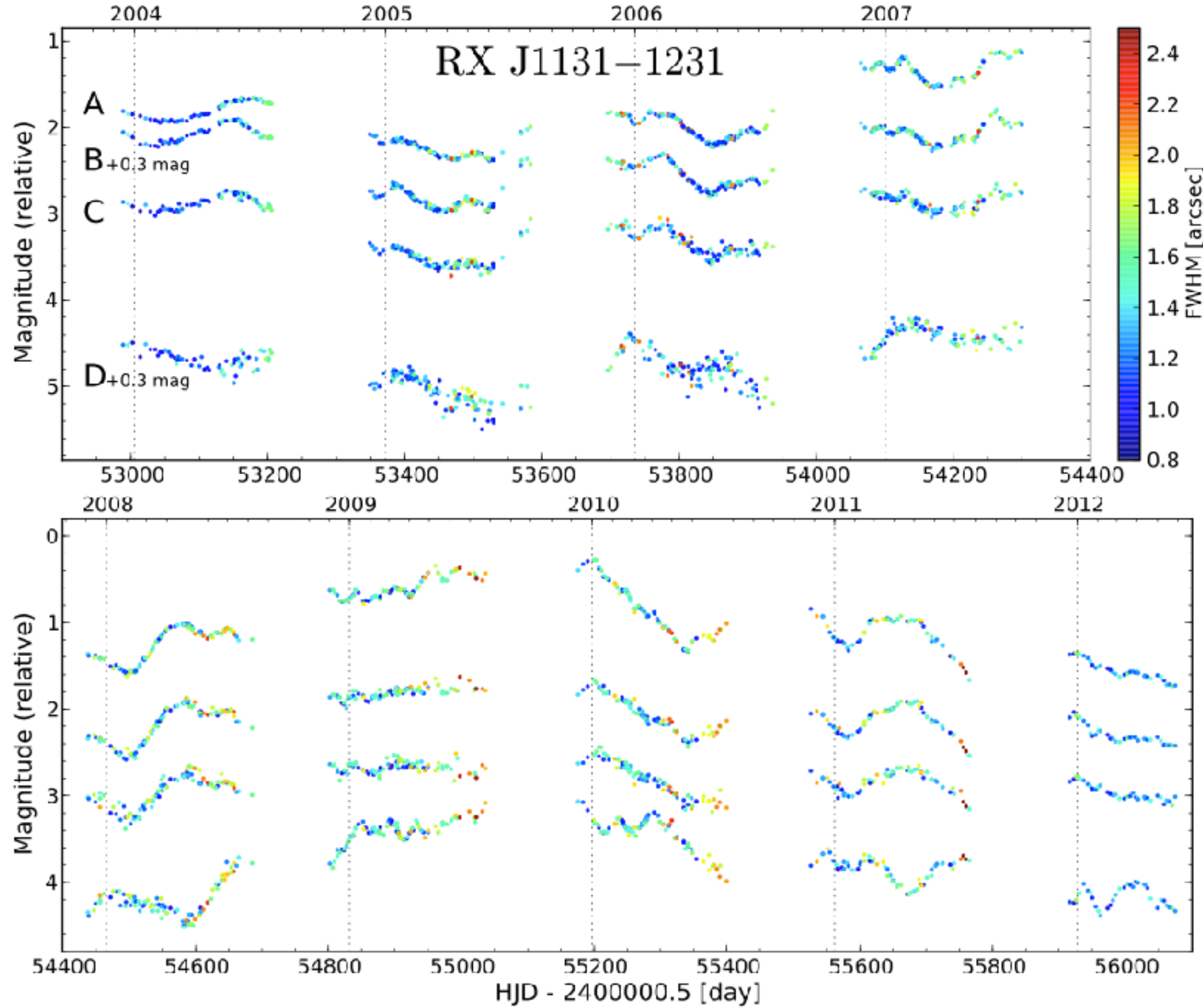


Euler deconvolved

Modeling of RX J1131-1231

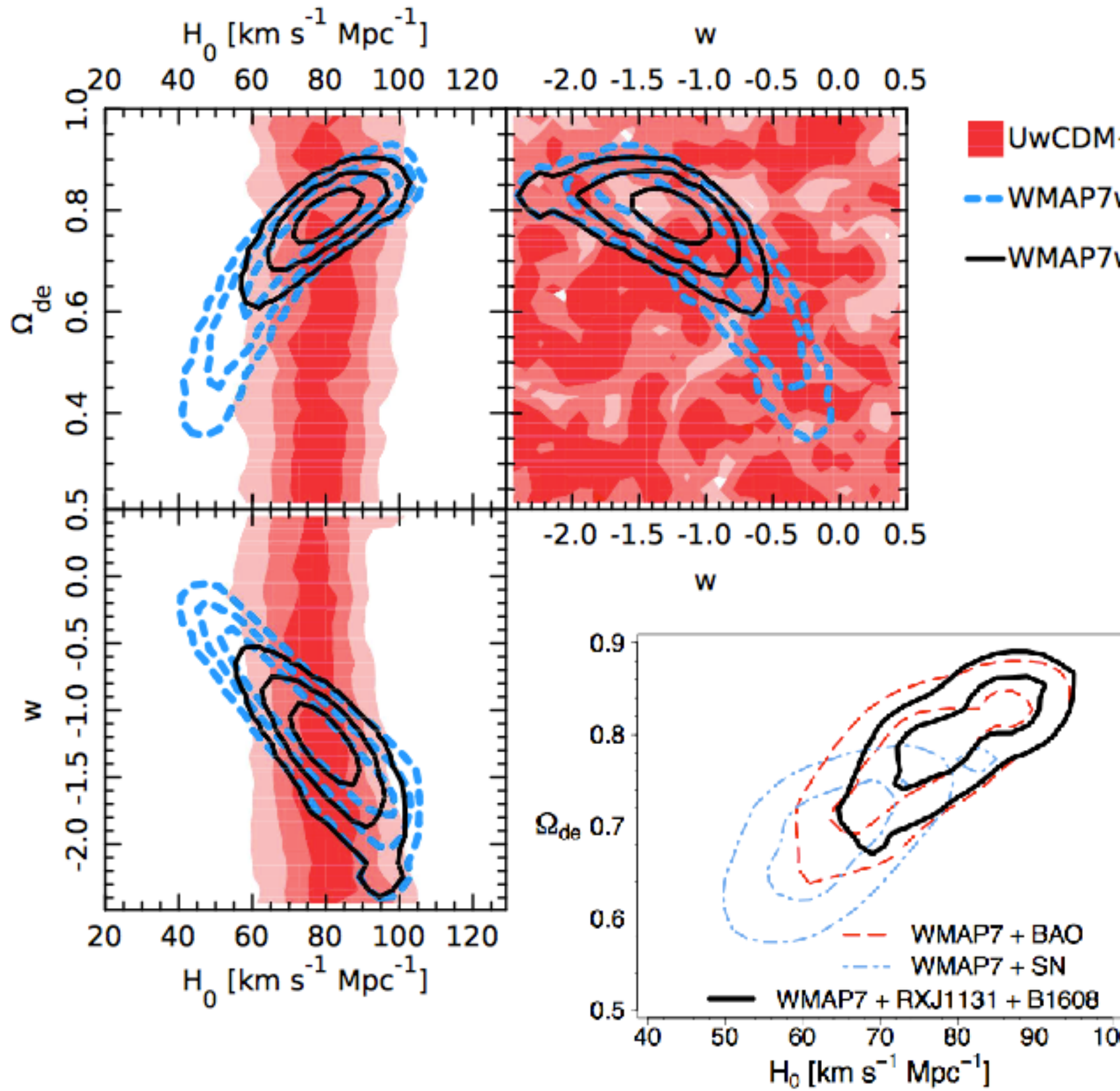


Curva de Luz de RX J1131-1231

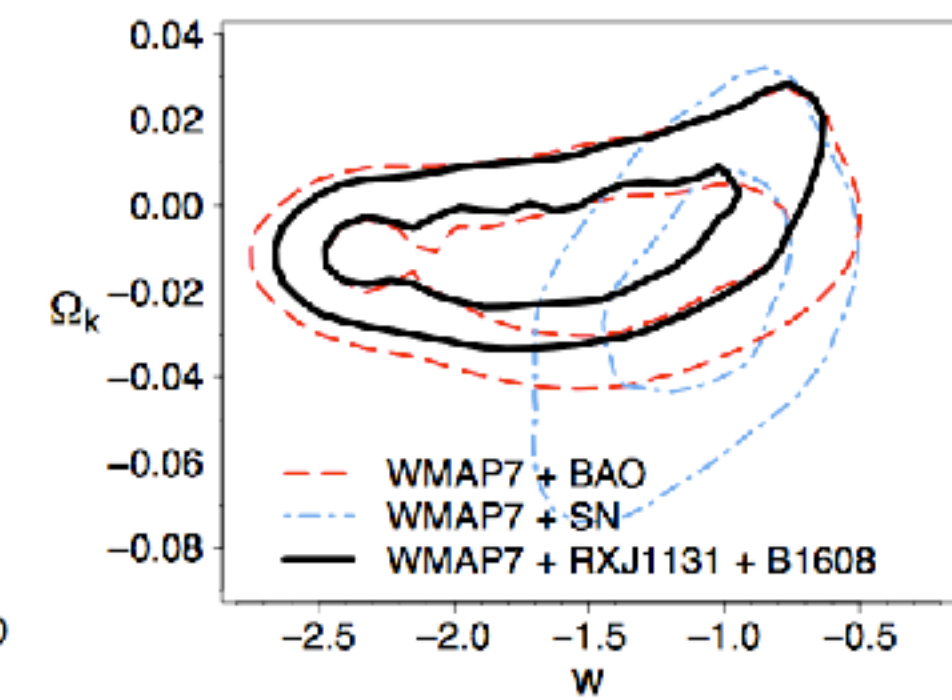


Tewes et al., COSMOGRAIL

Cosmological Constraints

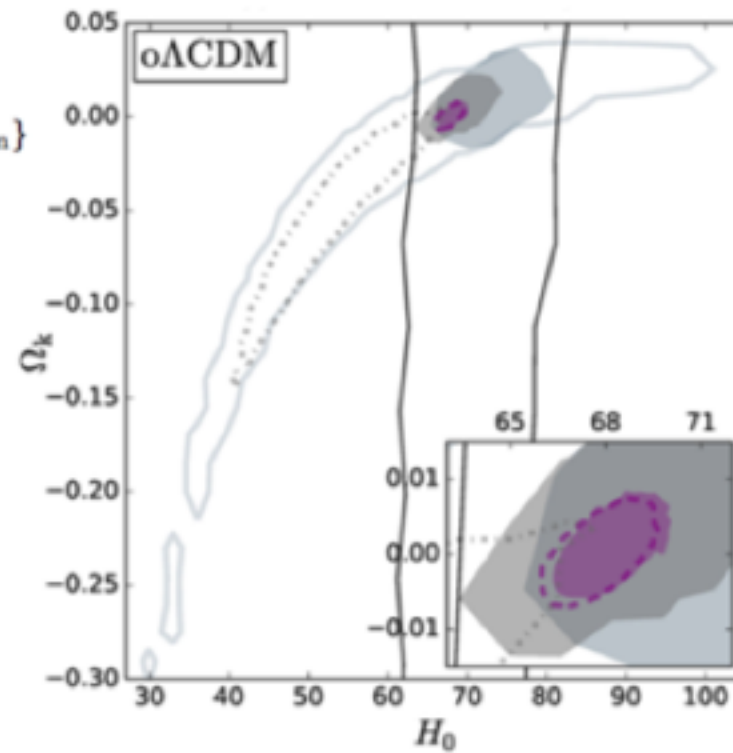


Suyu et al. 2012

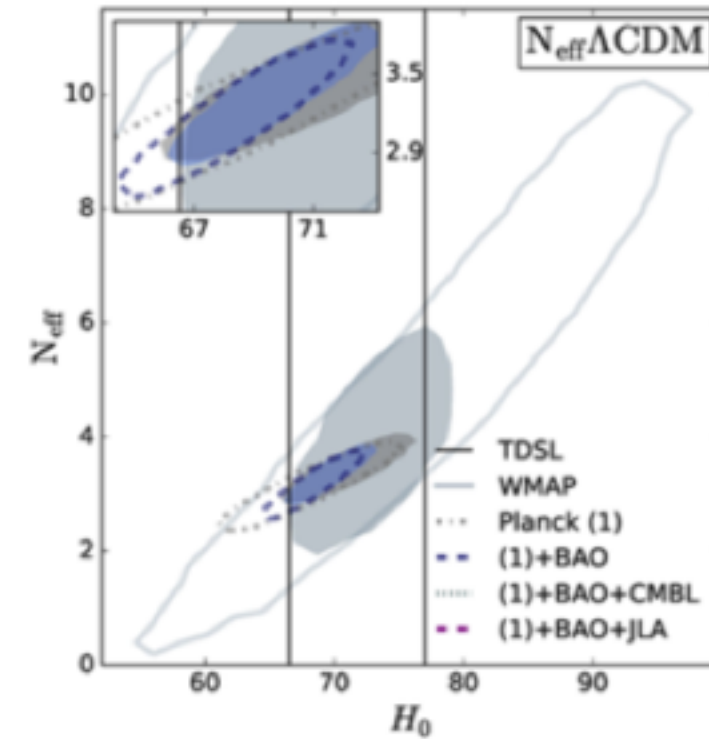


Cosmology Results

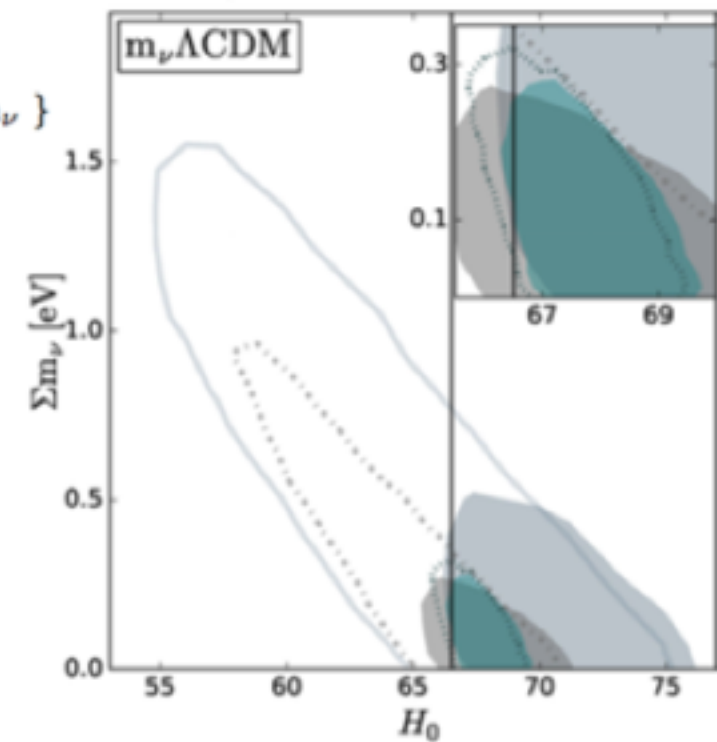
Non-flat Λ CDM cosmology
WMAP/Planck for $\{H_0, \Omega_\Lambda, \Omega_m\}$
 $\Omega_k = 1 - \Omega_\Lambda - \Omega_m$



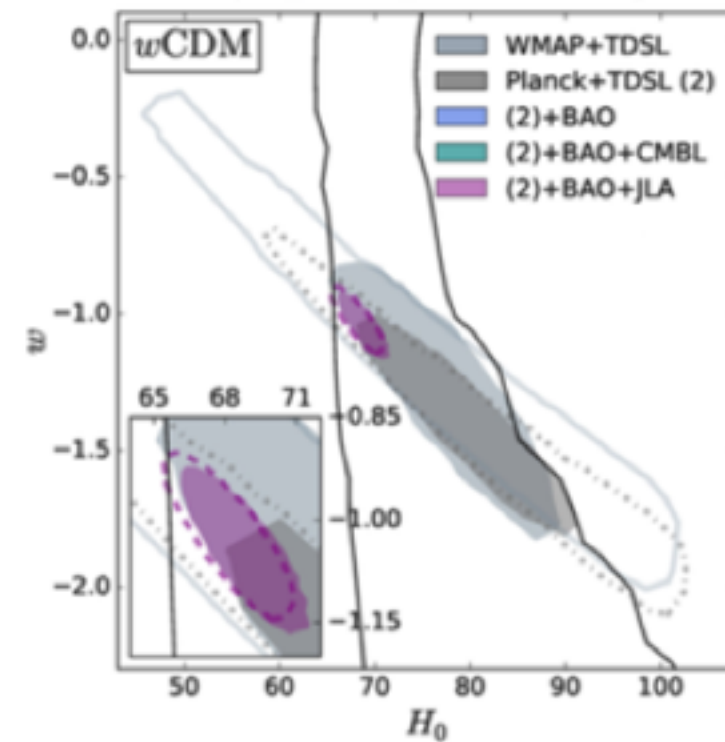
Flat Λ CDM cosmology
WMAP/Planck for $\{H_0, \Omega_\Lambda, N_{\text{eff}}\}$



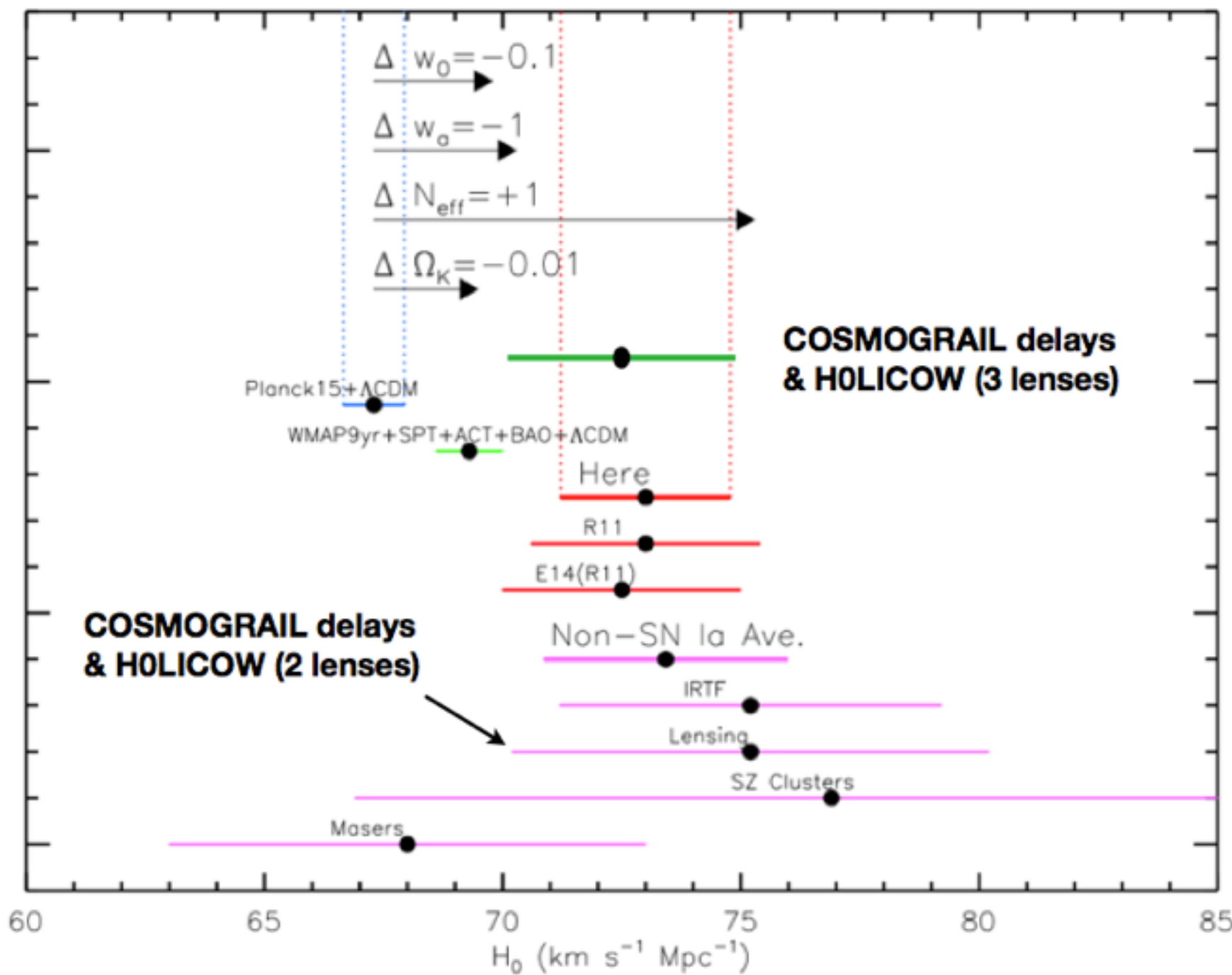
Flat Λ CDM cosmology
WMAP/Planck for $\{H_0, \Omega_\Lambda, \Sigma m_\nu\}$



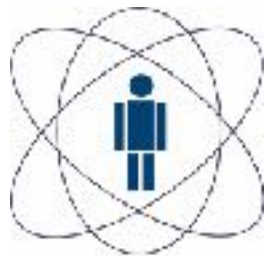
Flat w CDM cosmology
Planck for $\{H_0, w, \Omega_{de}\}$



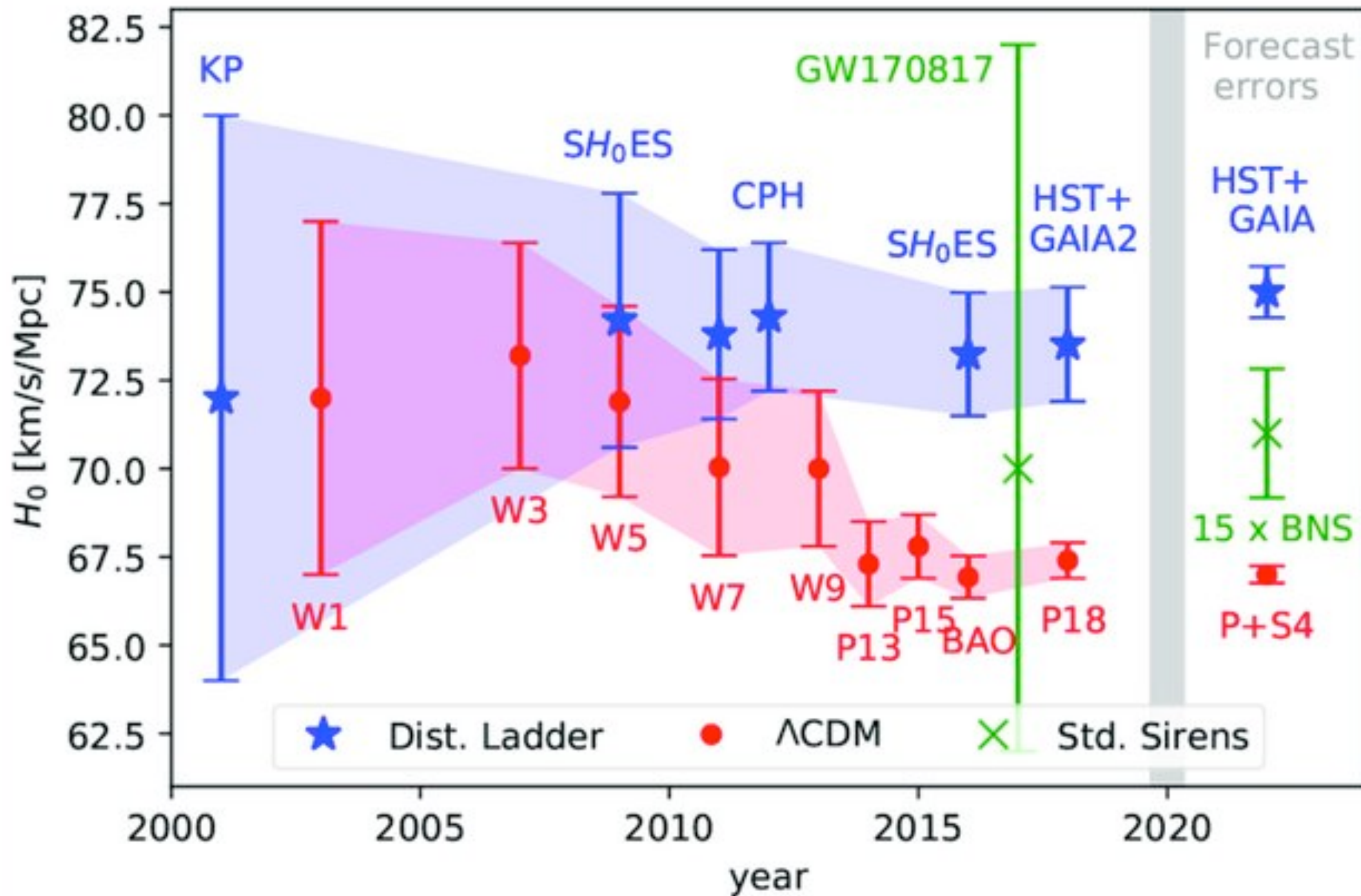
Comparison with other Cosmological Probes

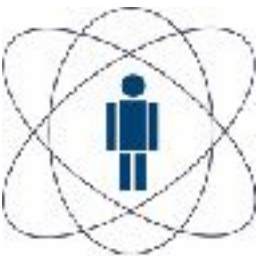


Adapted From Riess et al. (2016)

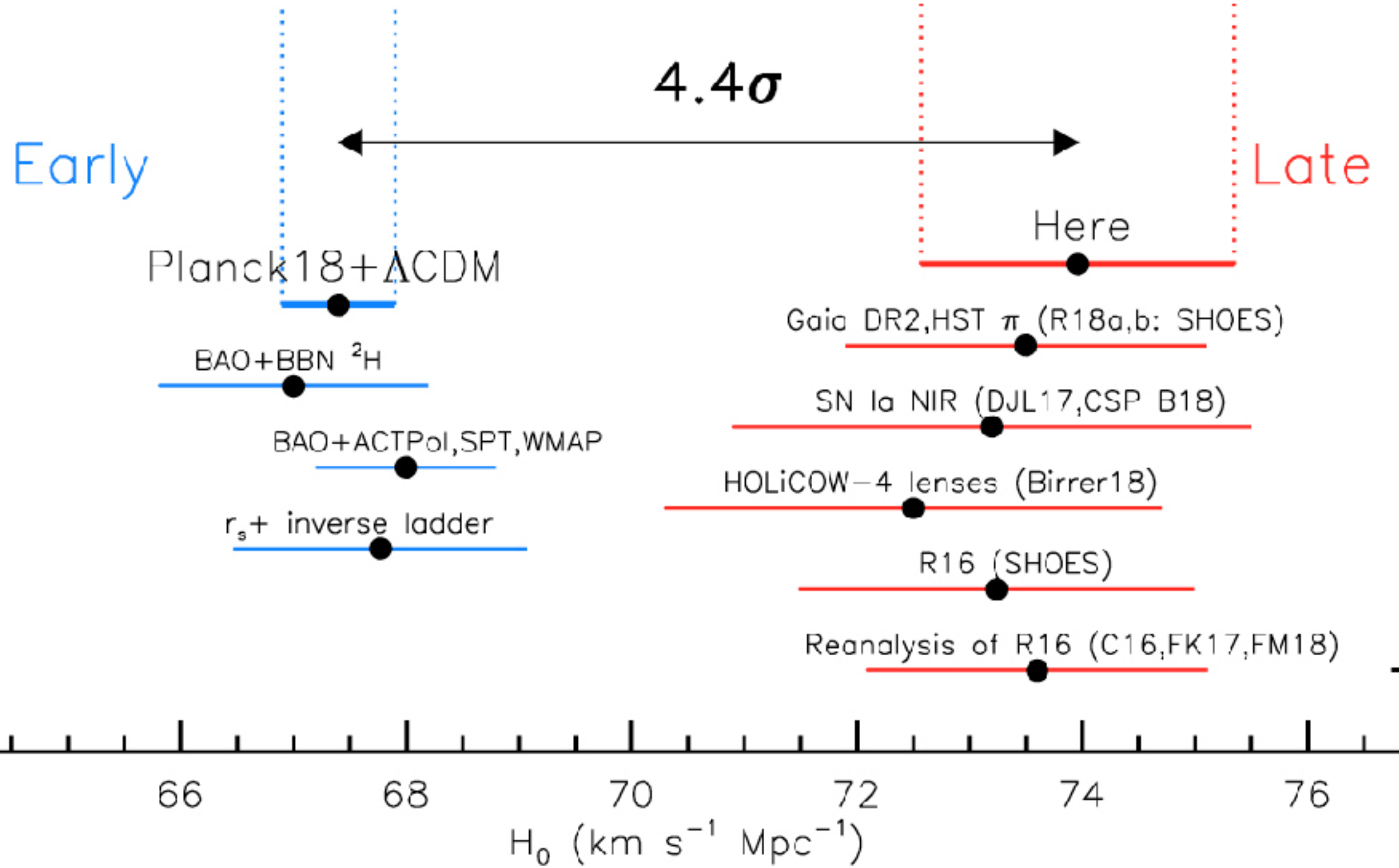


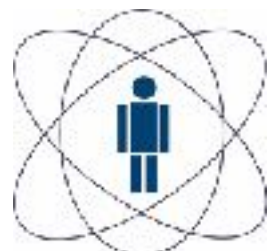
Tensão de Hubble



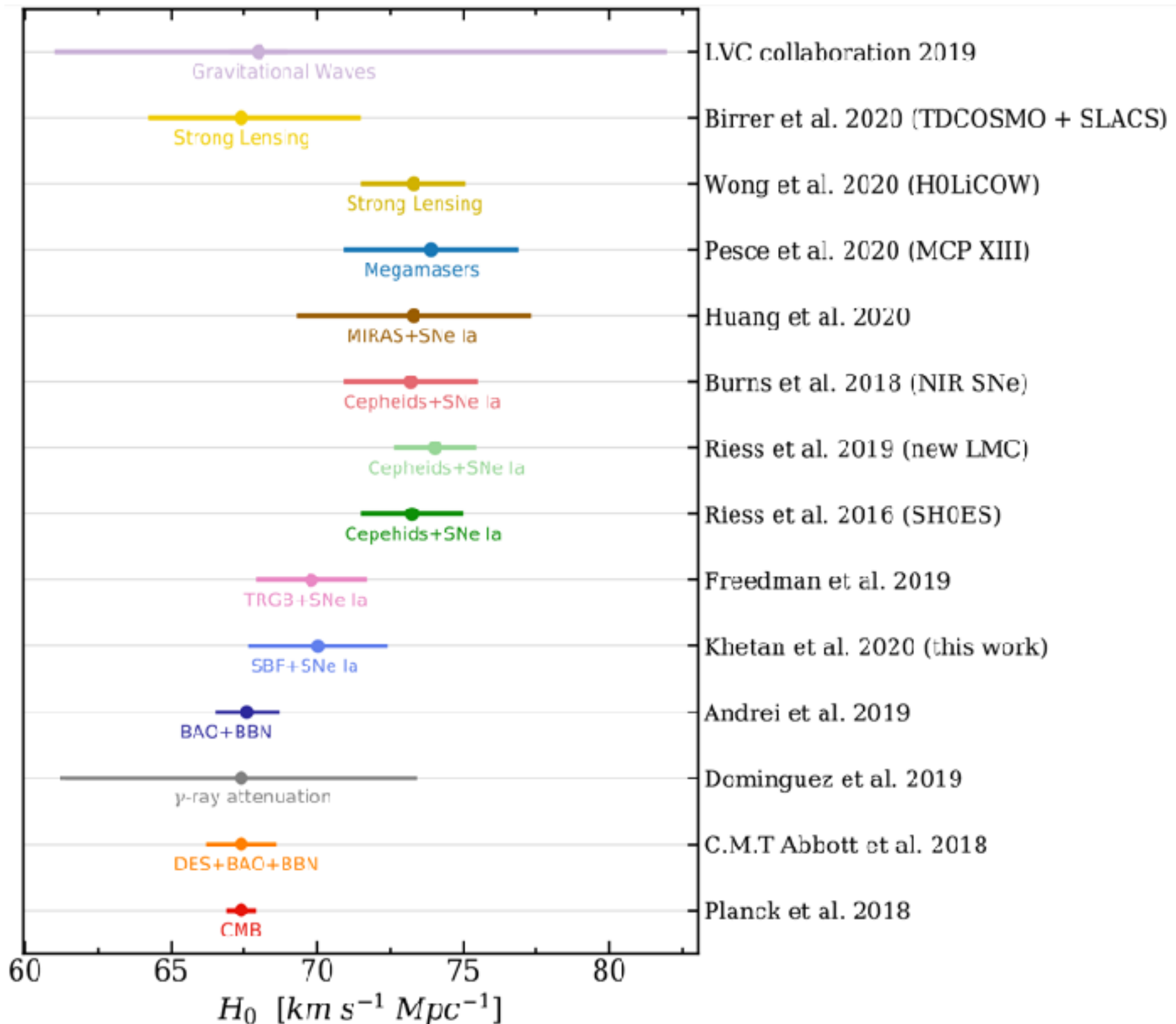


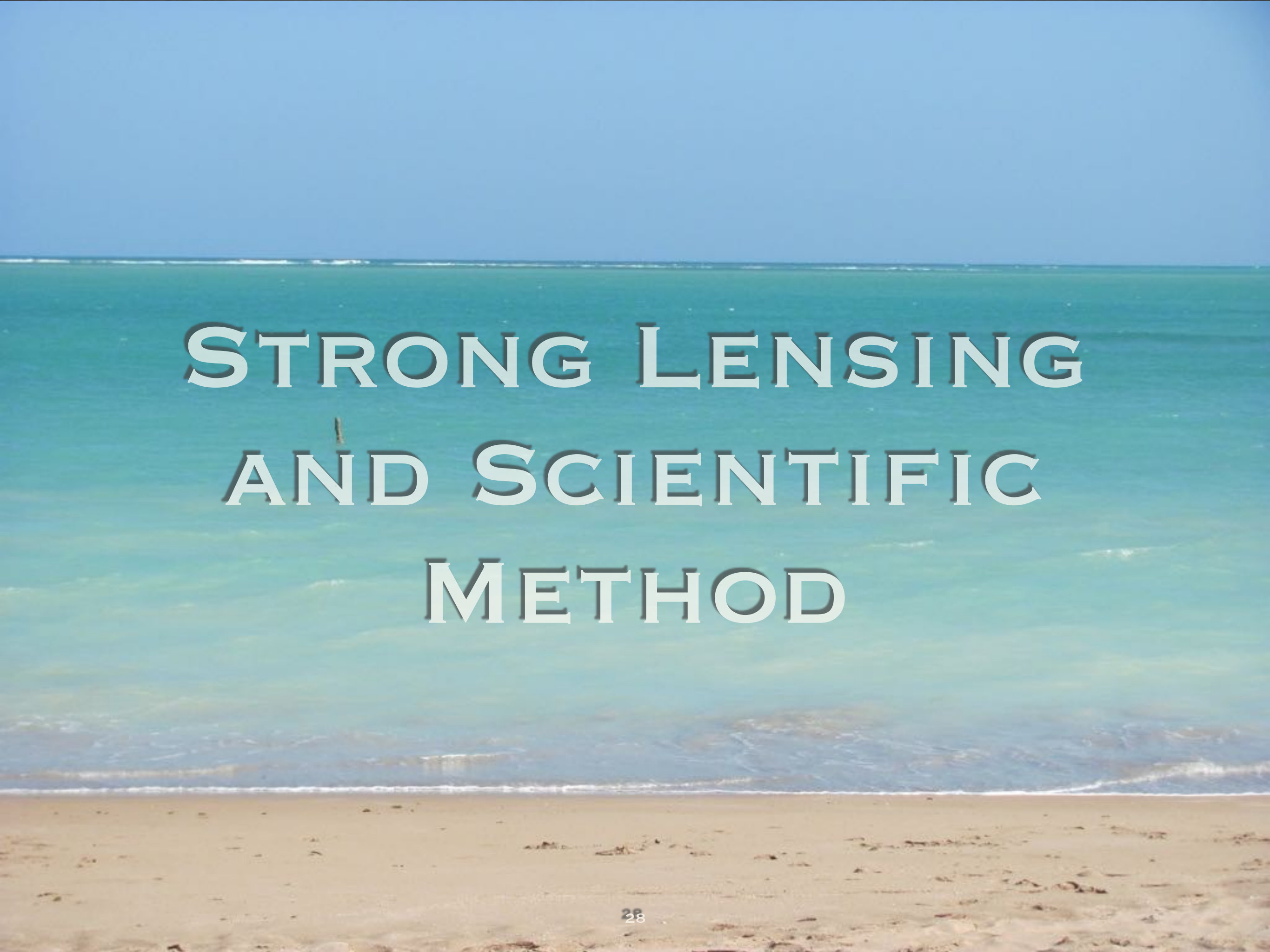
Tensão de Hubble



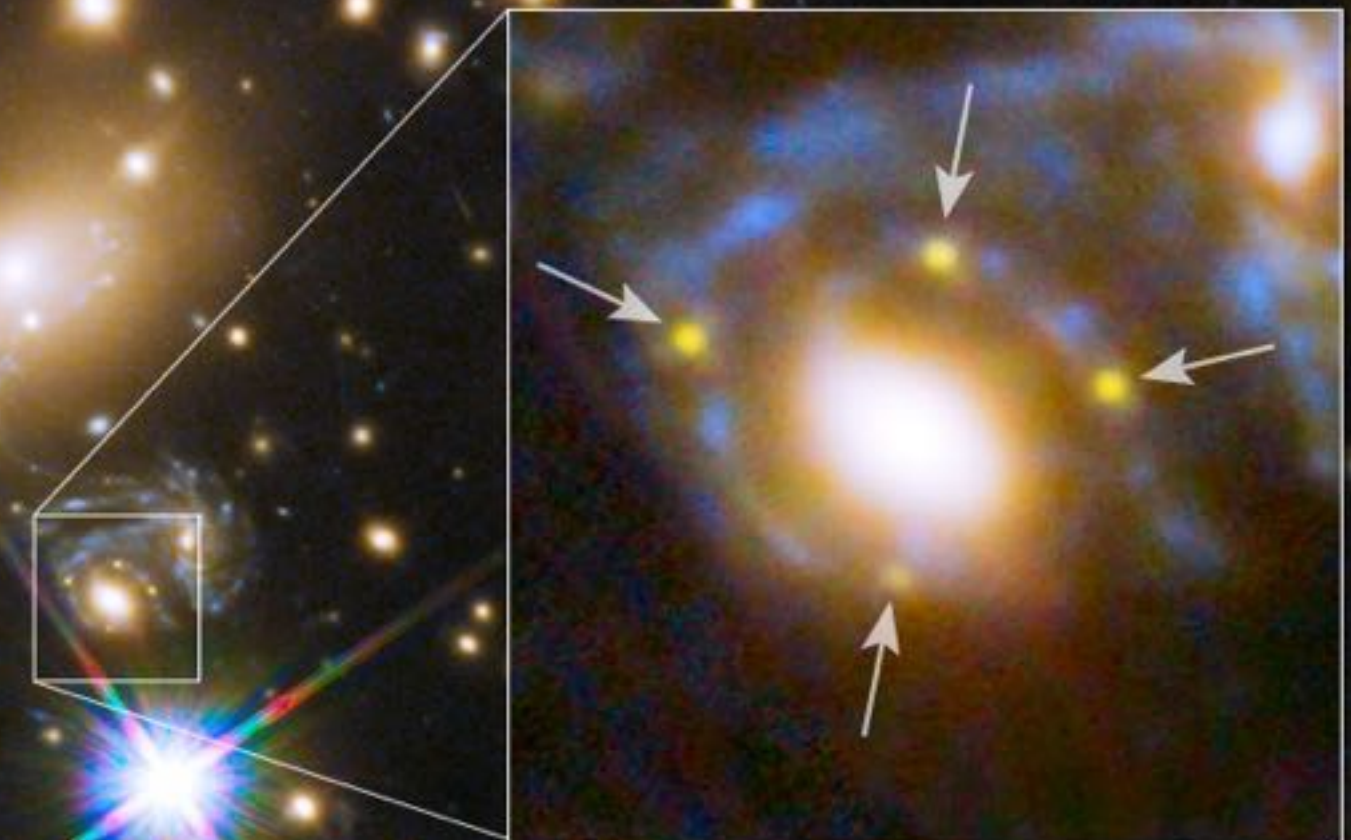
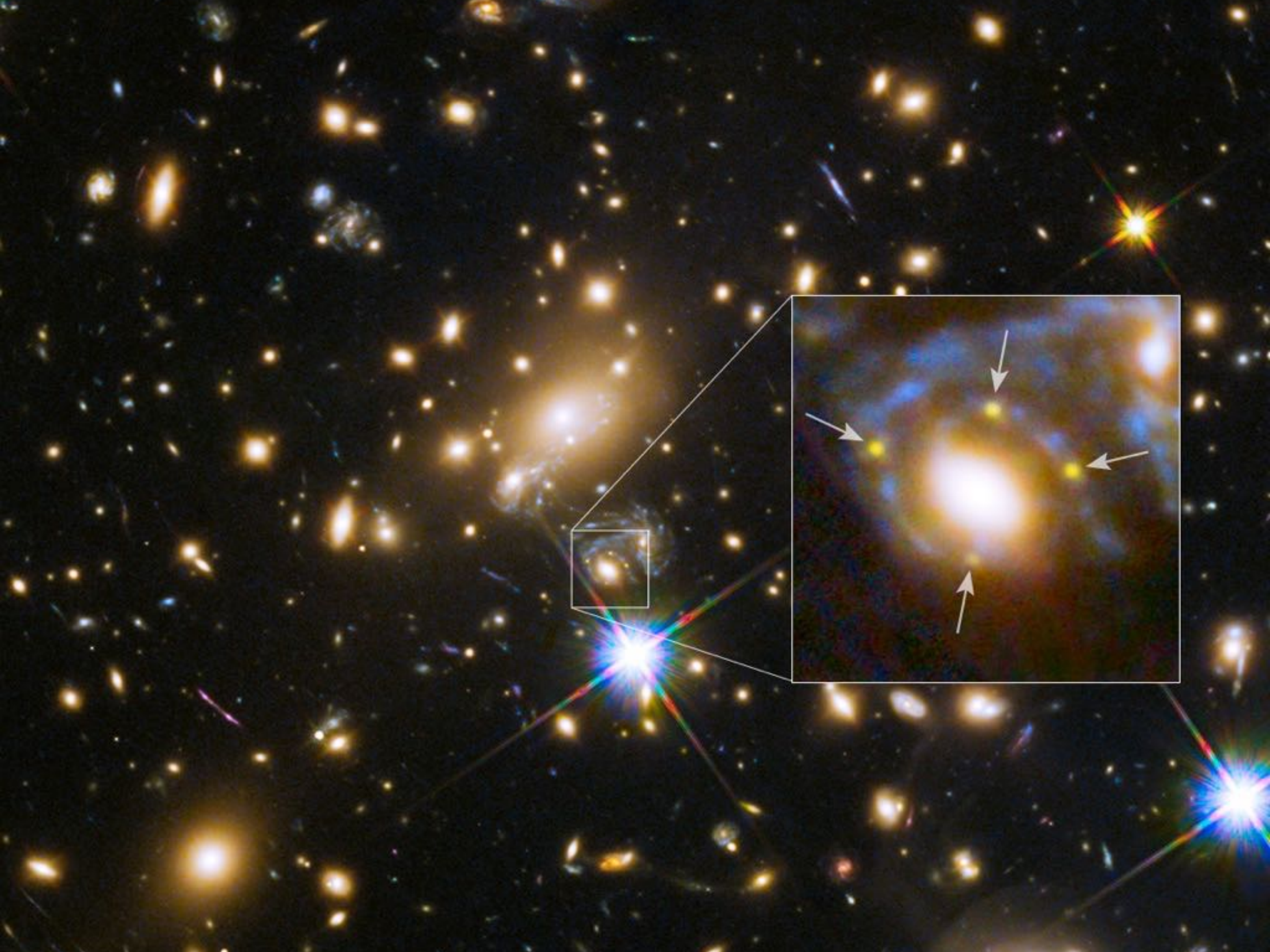


Tensão de Hubble

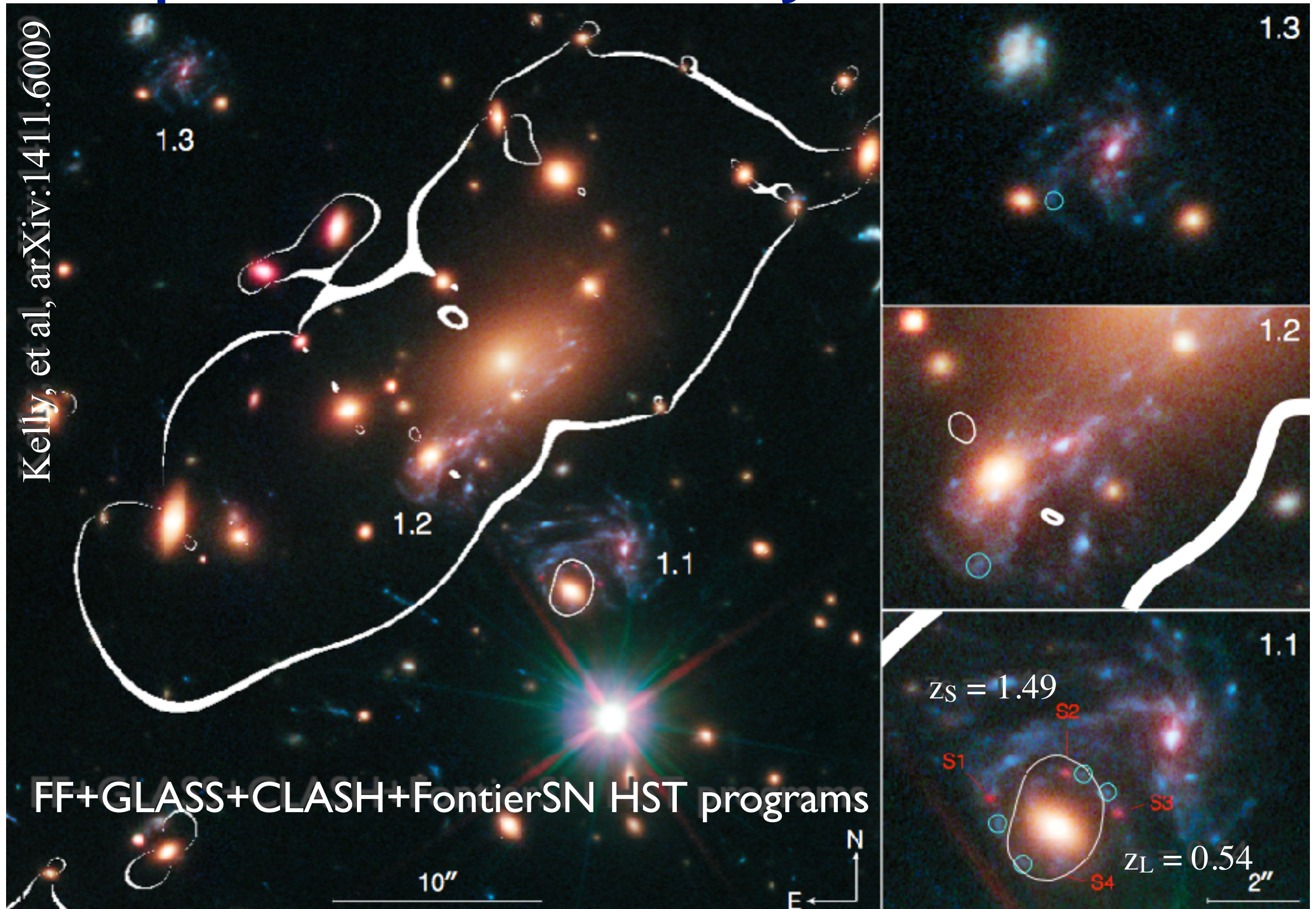


The background of the slide is a photograph of a tropical beach. The foreground is sandy, with some small debris scattered across it. The ocean in the middle ground is a vibrant turquoise color, with gentle white-capped waves breaking near the shore. The sky above is a clear, pale blue.

STRONG LENSING AND SCIENTIFIC METHOD



Supernova in MACS J1149.6+2223



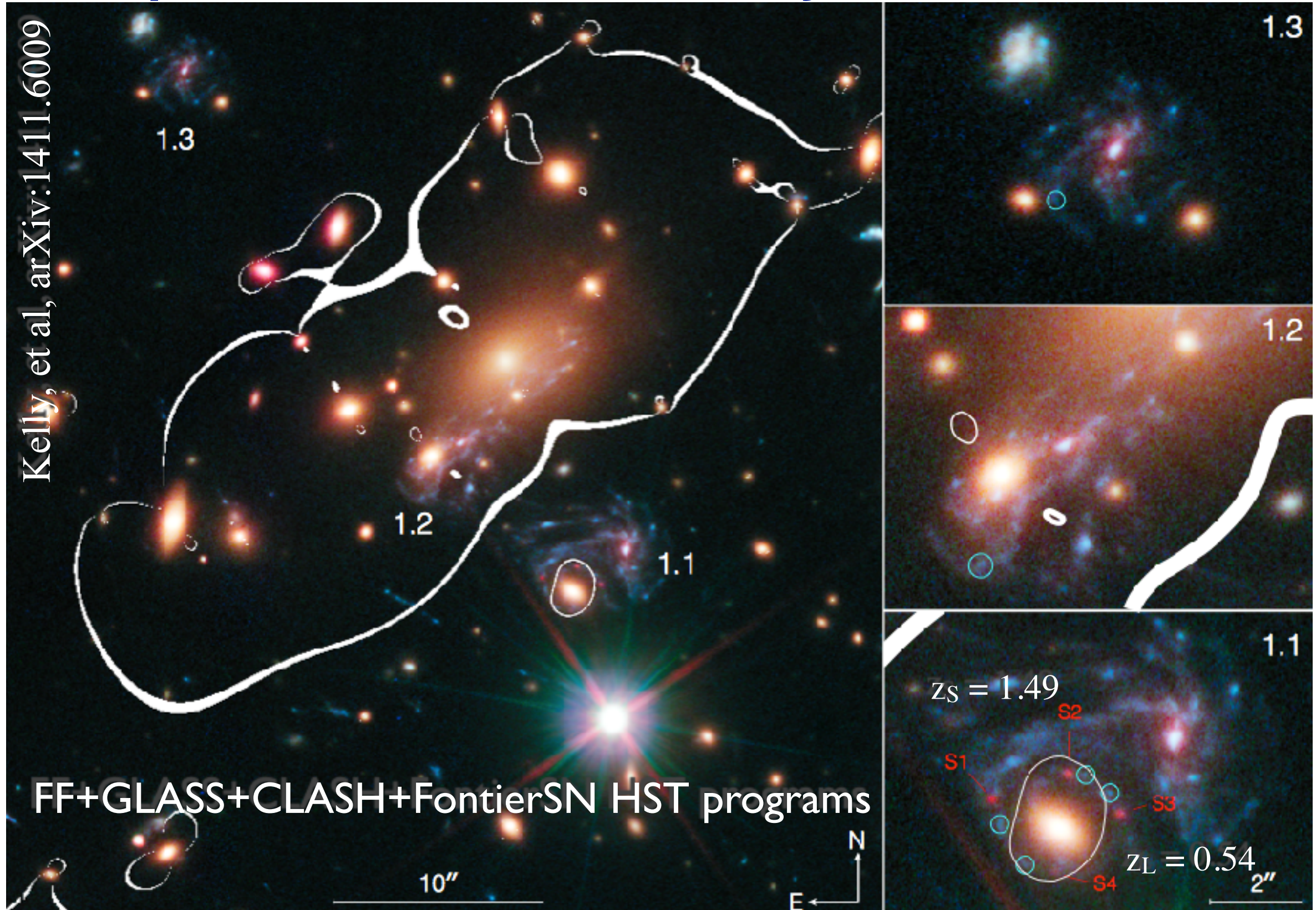
Multiple images by a galaxy cluster member
+ overall cluster potential

Can be modeled with
many degrees of freedom

Modeling Strong Lensing Clusters

- Use positions of multiple images/arcs
 - possibly: surface light distribution, relative fluxes
- Use positions and properties of the cluster galaxies
- Free parameters: 2D mass distribution!
- Parametric approach:
 - Dark matter halos: mass, shapes, number
 - Scaling relations for light - mass
- Can derive a lot of information
- But does it make sense?

Supernova em MACS J1149.6+2223



Use prediction for the appearance of multiple images to test the model

When Refsdal meets Popper!

THE STORY OF SUPERNOVA ‘REFSDAL’ TOLD BY MUSE*

C. GRILLO¹, W. KARMAN², S. H. SUYU³, P. ROSATI⁴, I. BALESTRA⁵, A. MERCURIO⁶, M. LOMBARDI⁷, T. TREU⁸,
G. B. CAMINHA⁴, A. HALKOLA, S. A. RODNEY^{9,10,11}, R. GAVAZZI¹², K. I. CAPUTI²

Draft version March 7, 2016

ABSTRACT

We present Multi Unit Spectroscopic Explorer (MUSE) observations in the core of the Hubble Frontier Fields (HFF) galaxy cluster MACS J1149.5+2223, where the first magnified and spatially-resolved multiple images of supernova (SN) ‘Refsdal’ at redshift 1.489 were detected. Thanks to a Director’s Discretionary Time program with the Very Large Telescope and the extraordinary efficiency of MUSE, we measure 117 secure redshifts with just 4.8 hours of total integration time on a single 1 arcmin² target pointing. We spectroscopically confirm 68 galaxy cluster members, with redshift values ranging from 0.5272 to 0.5660, and 18 multiple images belonging to 7 background, lensed sources distributed in redshifts between 1.240 and 3.703. Starting from the combination of our catalog with those obtained from extensive spectroscopic and photometric campaigns using the *Hubble Space Telescope*, we select a sample of 300 (164 spectroscopic and 136 photometric) cluster members, within approximately 500 kpc from the brightest cluster galaxy, and a set of 88 reliable multiple images associated to 10 different background source galaxies and 18 distinct knots in the spiral galaxy hosting SN ‘Refsdal’. We exploit this valuable information to build 6 detailed strong lensing models, the best of which reproduces the observed positions of the multiple images with a root-mean-square offset of only 0.26''. We use these models to quantify the statistical and systematic errors on the predicted values of magnification and time delay of the next emerging image of SN ‘Refsdal’. We find that its peak luminosity should occur between March and June 2016, and should be approximately 20% fainter than the dimmest (S4) of the previously detected images but above the detection limit of the planned *HST*/WFC3 follow-up. We present our two-dimensional reconstruction of the cluster mass density distribution and of the SN ‘Refsdal’ host galaxy surface brightness distribution. We outline the roadmap towards even better strong lensing models with a synergetic MUSE and *HST* effort.

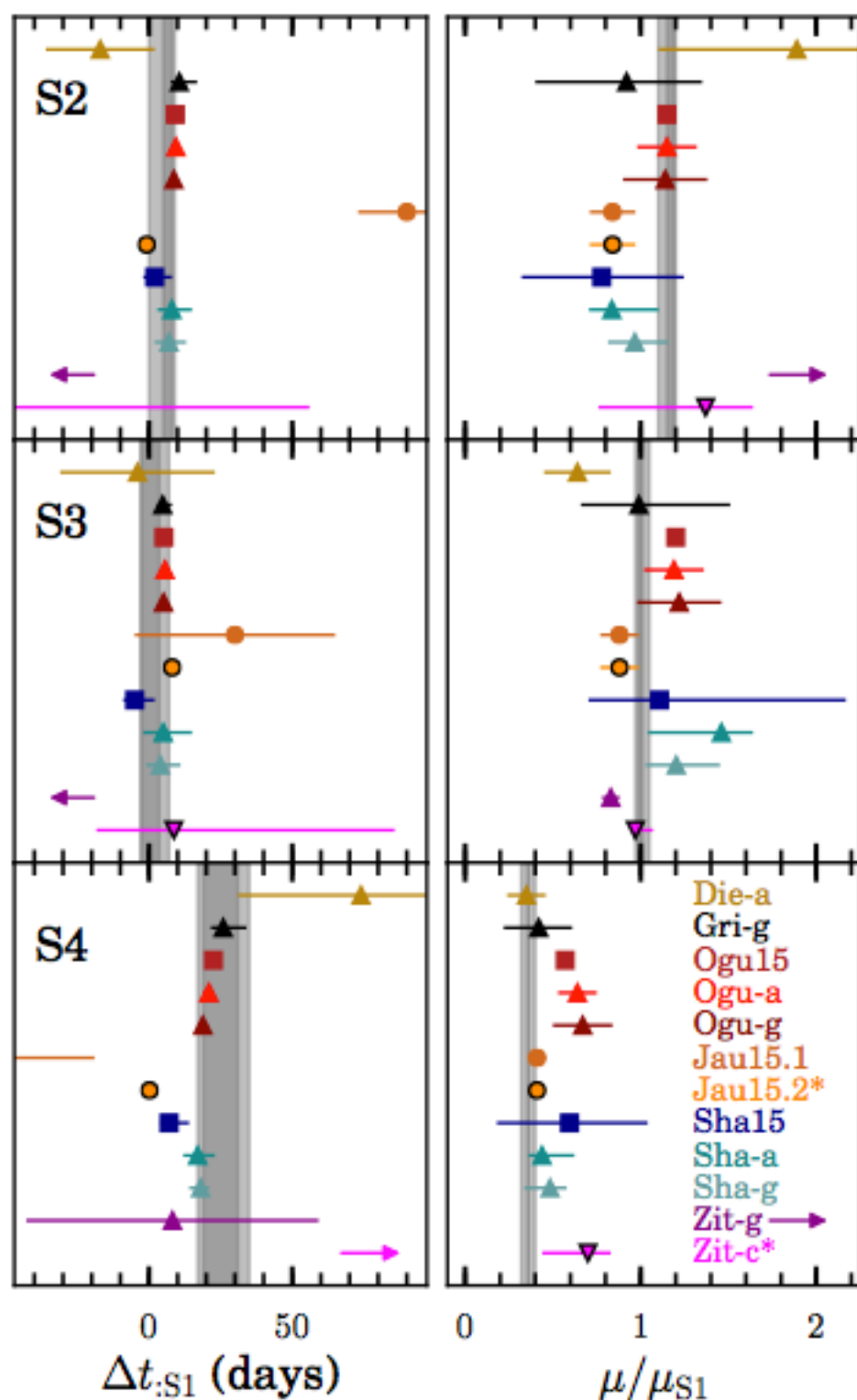
Subject headings: gravitational lensing – galaxies: clusters: general – galaxies: clusters: individuals: MACS J1149.5+2223 – Dark matter

"REFSDAL" MEETS POPPER: COMPARING PREDICTIONS OF THE RE-APPEARANCE OF THE MULTIPLY IMAGED SUPERNOVA BEHIND MACSJ1149.5+2223

T. Treu^{1,2*}, G. Brammer², J. M. Diego³, C. Grillo⁴, P. L. Kelly⁵, M. Oguri^{6,7†}, K. Sharon¹², A. Zitrin^{13,29} Show full author list

Published 2016 January 20 • © 2016. The American Astronomical Society. All rights reserved.

The Astrophysical Journal, Volume 817, Number 1



A free-form prediction for the reappearance of supernova Refsdal in the Hubble Frontier Fields cluster MACSJ1149.5+2223

Jose M. Diego,^{1,2*} Tom Broadhurst,^{2,3} Cuncheng Chen,⁴ Jeremy Lim,⁴ Adi Zitrin,^{5,†} Brian Chan,⁴ Dan Coe,⁶ Holland C. Ford,⁶ Daniel Lam⁴ and Wei Zheng⁶

¹IICA, Instituto de Física de Cantabria (UC-CSIC), Av. de Los Castros s/n, E-39005 Santander, Spain

²Fisika Teorikoa, Zientzia eta Teknologia Fakultatea, Euskal Herriko Unibertsitatea UPV/EHU, E-48080 Bilbao, Spain

³IKERBASQUE, Basque Foundation for Science, Alameda Urquiza 36-3, E-48008 Bilbao, Spain

⁴Department of Physics, The University of Hong Kong, 0960-0002-6535-5575, Pokfulam Road, Hong Kong

⁵Cahill Center for Astronomy and Astrophysics, California Institute of Technology, MS 249-17, Pasadena, CA 91125, USA

⁶Department of Physics and Astronomy, Johns Hopkins University, Baltimore, MD 21218, USA

THE STORY OF SUPERNOVA 'REFSDAL' TOLD BY MUSE*

C. GRILLO¹, W. KARMAN², S. H. SUYU³, P. ROSATI⁴, I. BALESTRA⁵, A. MERCURIO⁶, M. LOMBARDI⁷, T. TREU⁸, G. B. CAMINHA⁹, A. HALKOLA¹⁰, S. A. RODNEY^{9,10,11}, R. GAVAZZI¹², K. I. CAPUTI²

Draft version March 7, 2016

Monthly Notices
of the
ROYAL ASTRONOMICAL SOCIETY
MNRAS 457, 2029–2042 (2016)

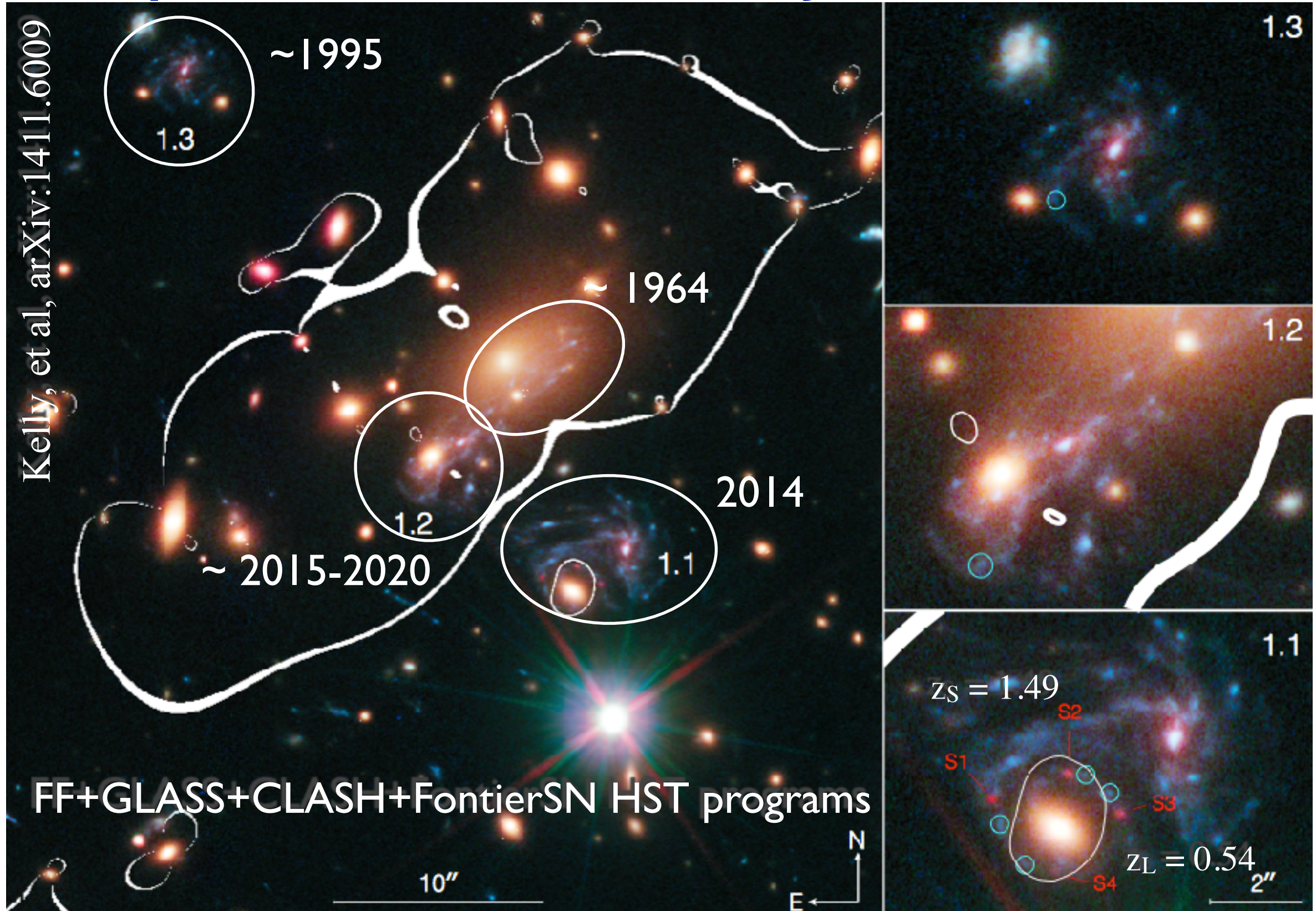
doi:10.1093/mnras/stw069

Hubble Frontier Fields: predictions for the return of SN Refsdal with the MUSE and GMOS spectrographs

M. Jauzac,^{1,2,3*} J. Richard,⁴ M. Limousin,⁵ K. Knowles,³ G. Mahler,⁴ G. P. Smith,⁶ J.-P. Kneib,^{5,7} E. Jullo,⁵ P. Natarajan,⁸ H. Ebeling,⁹ H. Attek,⁸ B. Clément,⁴ D. Eckert,¹⁰ E. Egami,¹¹ R. Massey^{1,2} and M. Rexroth⁷

of MACS J0416.1–2403 and Abell 2744. In light of the discovery of the first resolved quadruply lensed supernova, SN Refsdal, in one of the multiply imaged galaxies identified in MACS J1149, we use our revised mass model to investigate the time delays and predict the rise of the next image between 2015 November and 2016 January.

Supernova em MACSJ1149.6+2223

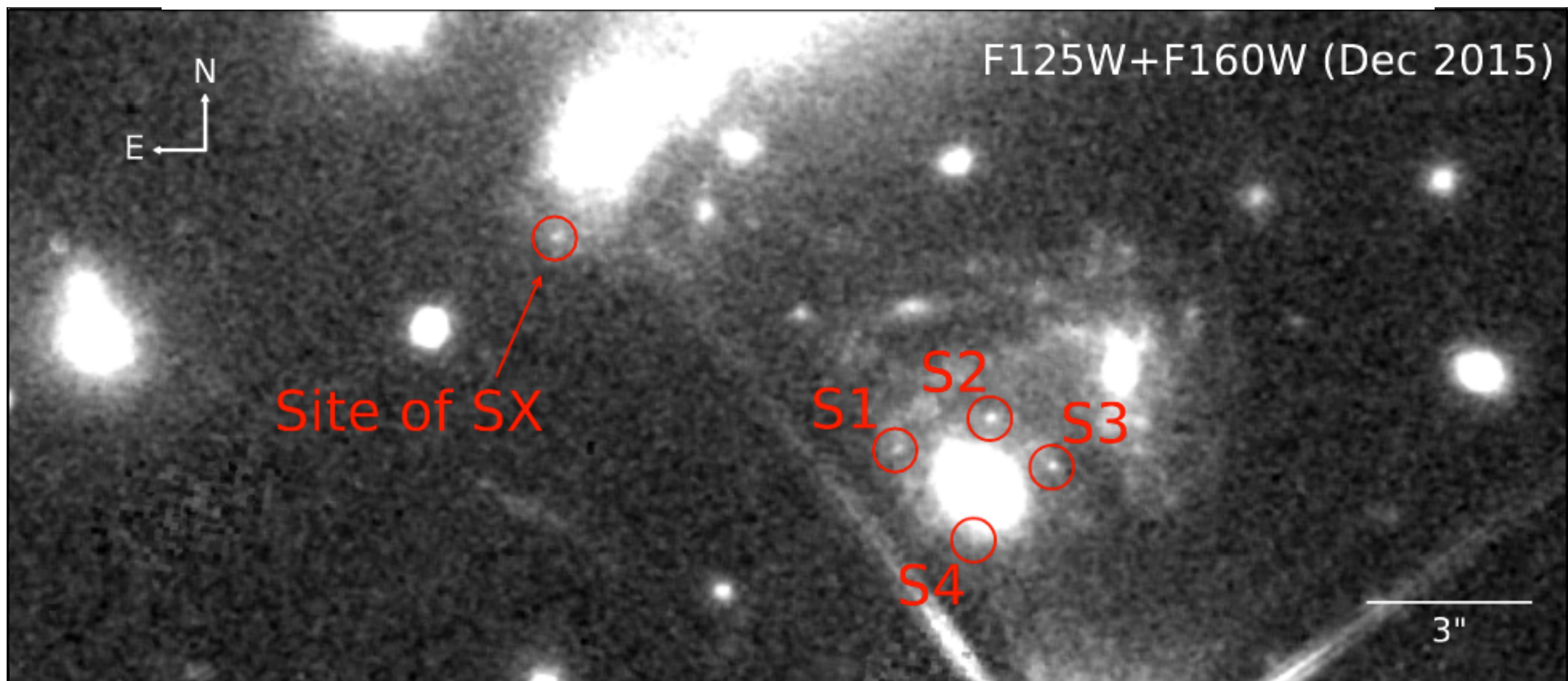


DEJA VU ALL OVER AGAIN: THE REAPPEARANCE OF SUPERNOVA REFSDAL

P. L. Kelly¹, S. A. Rodney², T. Treu^{3,3}, L.-G. Strolger⁴, R. J. Foley^{5,6}, S. W. Jha⁷, J. Selsing⁸, G. Brammer⁴, M. Bradač⁹, S. B. Cenko^{10,11} [Show full author list](#)

Published 2016 February 24 • © 2016. The American Astronomical Society. All rights reserved.

[The Astrophysical Journal Letters, Volume 819, Number 1](#)

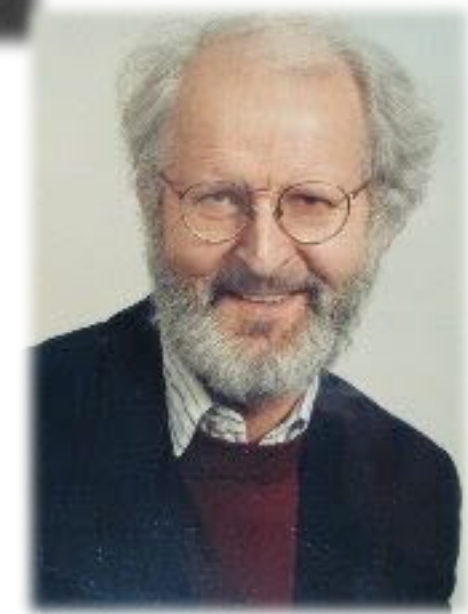
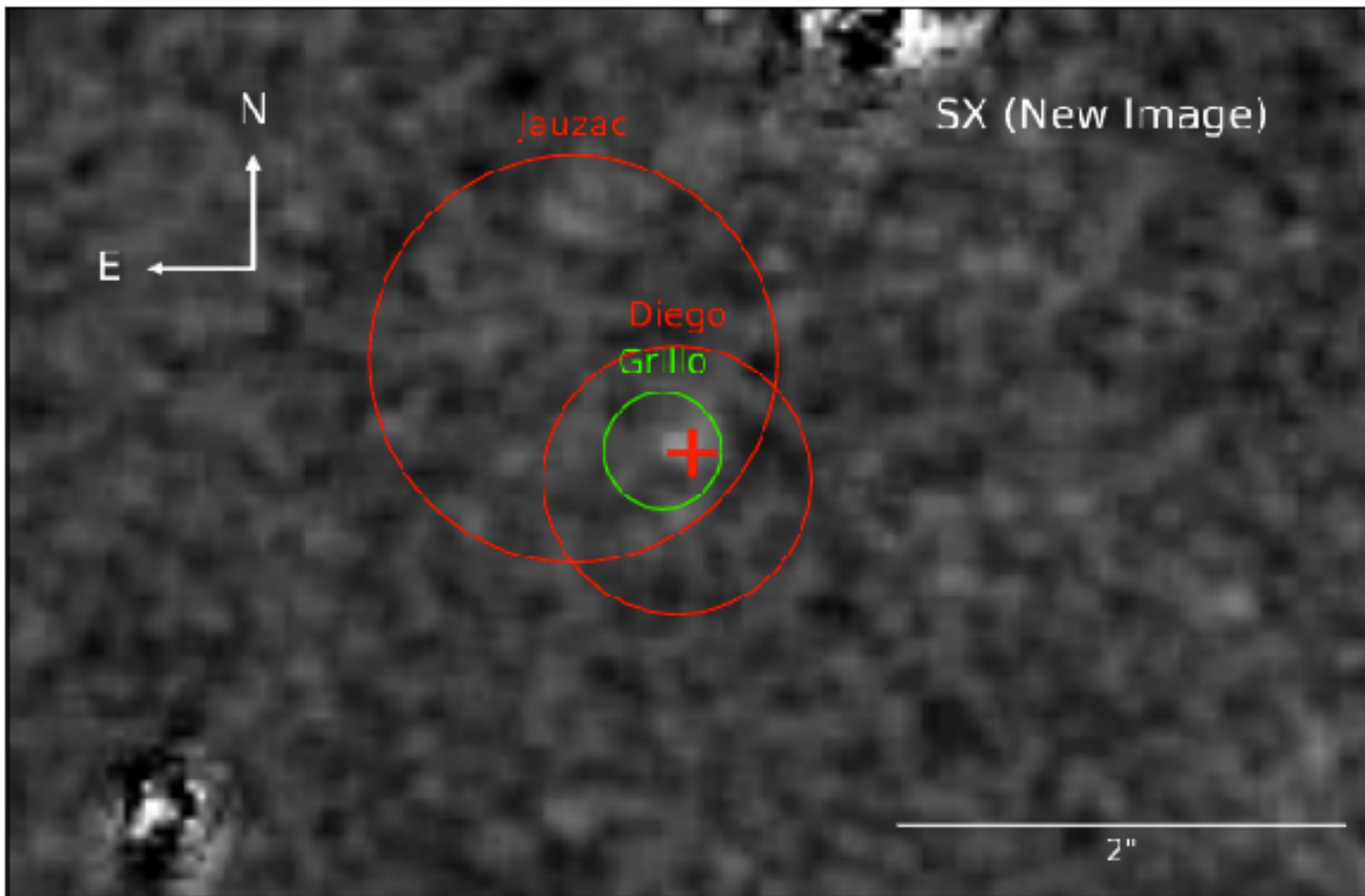


DEJA VU ALL OVER AGAIN: THE REAPPEARANCE OF SUPERNOVA REFSDAL

P. L. Kelly¹, S. A. Rodney², T. Treu^{3,3}, L.-G. Strolger⁴, R. J. Foley^{5,6}, S. W. Jha⁷, J. Selsing⁸, G. Brammer⁴, M. Bradač⁹, S. B. Cenko^{10,11} [Show full author list](#)

Published 2016 February 24 • © 2016. The American Astronomical Society. All rights reserved.

[The Astrophysical Journal Letters, Volume 819, Number 1](#)



MASS DISTRIBUTION FROM STRONG LENSING

► Constraints on the particle properties of Dark Matter

► Density profiles of galaxies and inner cluster regions:

► cuspy halo profiles? $\rho(r) \propto r^{-\gamma}$ $\gamma \sim 1$ Bartelmann, astro-ph/0207032

► baryonic processes: cooling, AGN feedback,... Mead et al. 1001.2281

► dark matter interactions

► Substructure Moustakas et al. 0902.3219, Koopmans et al. 0902.3186

► overabundance of satellites

► primordial spectrum

► Luminous x Matter

► e.g. DM cross section Williams and Saha, 1102.3943



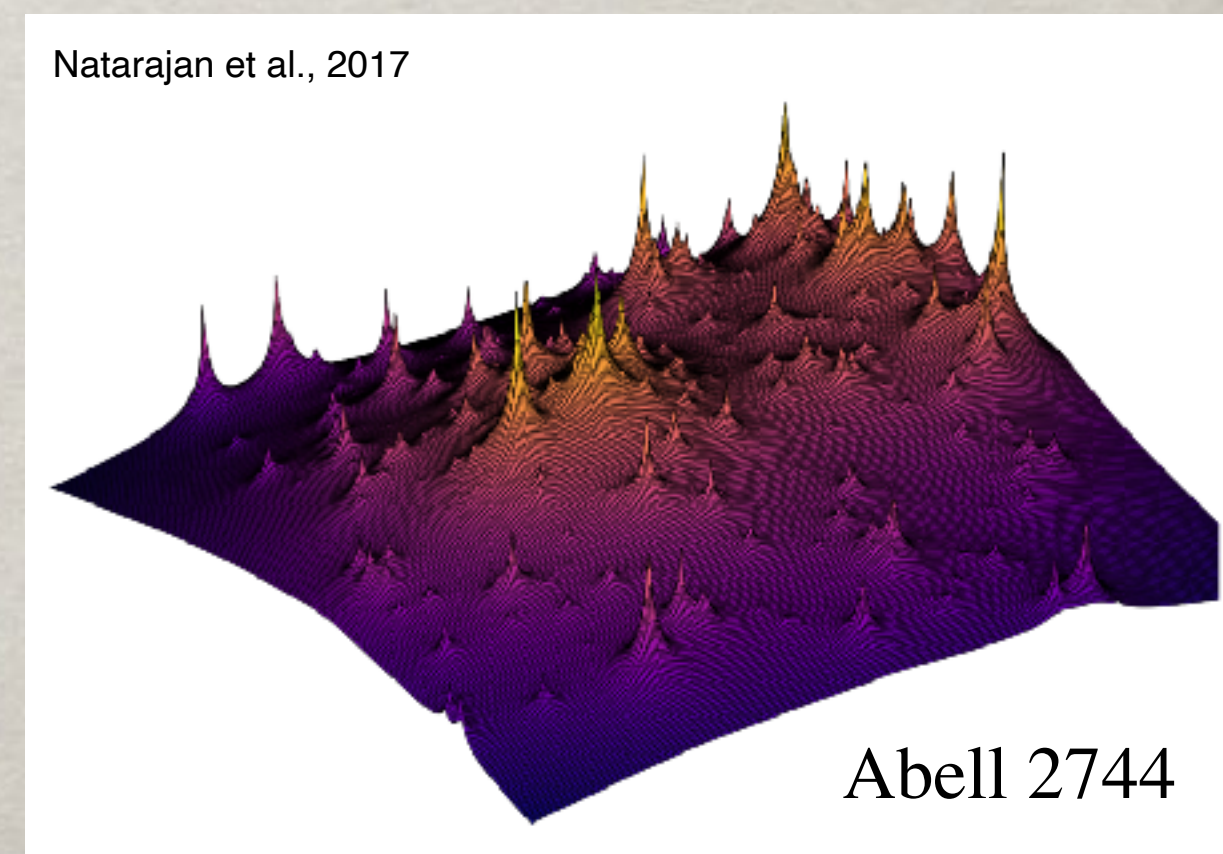
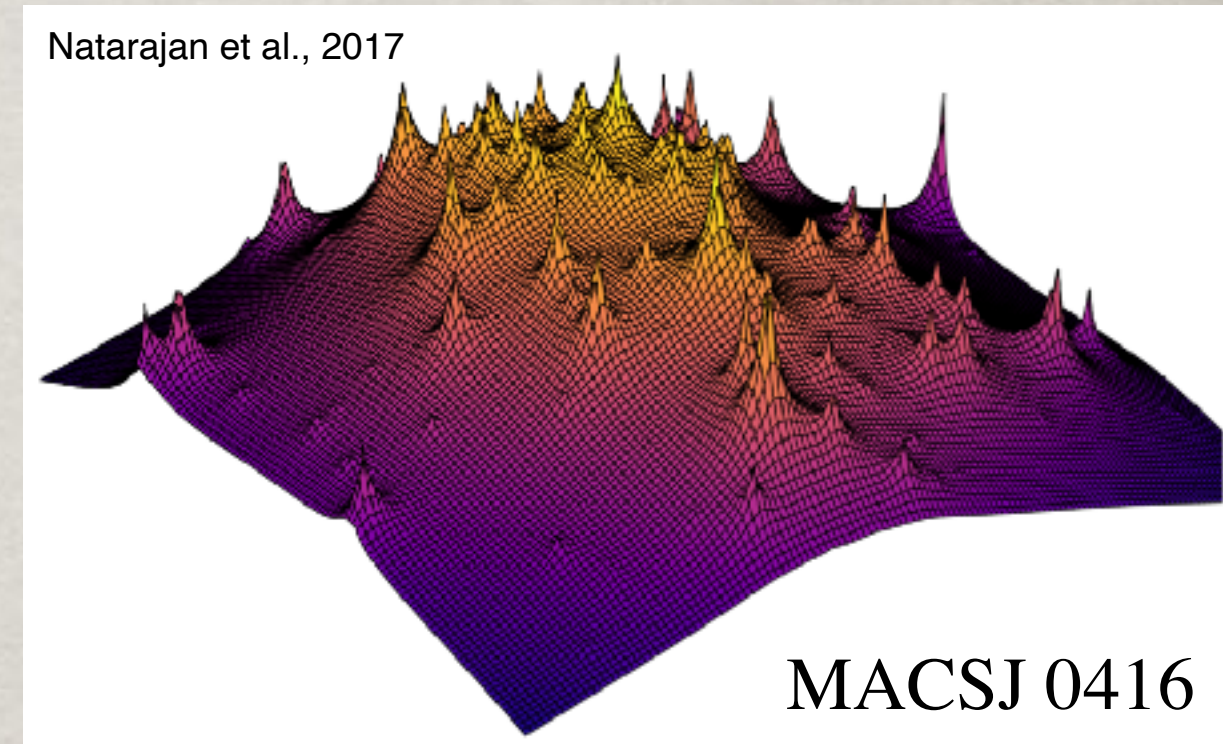
Strong Lensing and Dark Matter

- Large-scale Geometry
 - Background cosmology: Ω_M
- Lens potential: Mass distribution
 - Dark Matter abundance and distribution
 - Primordial spectrum (mass)
 - Self-interaction
- Gravitational telescope
 - $z \sim 2$ – details of highly magnified galaxies (resolved!)
 - $z \sim 6$ – galaxy abundance at high- z
- Challenges:
 - High-resolution, deep imaging; spectroscopy (including IFU)
 - Finding Strong Lenses (specially “golden lenses”)
 - Systematics

Direct detection of substructure in clusters

Sub-halo power spectrum:

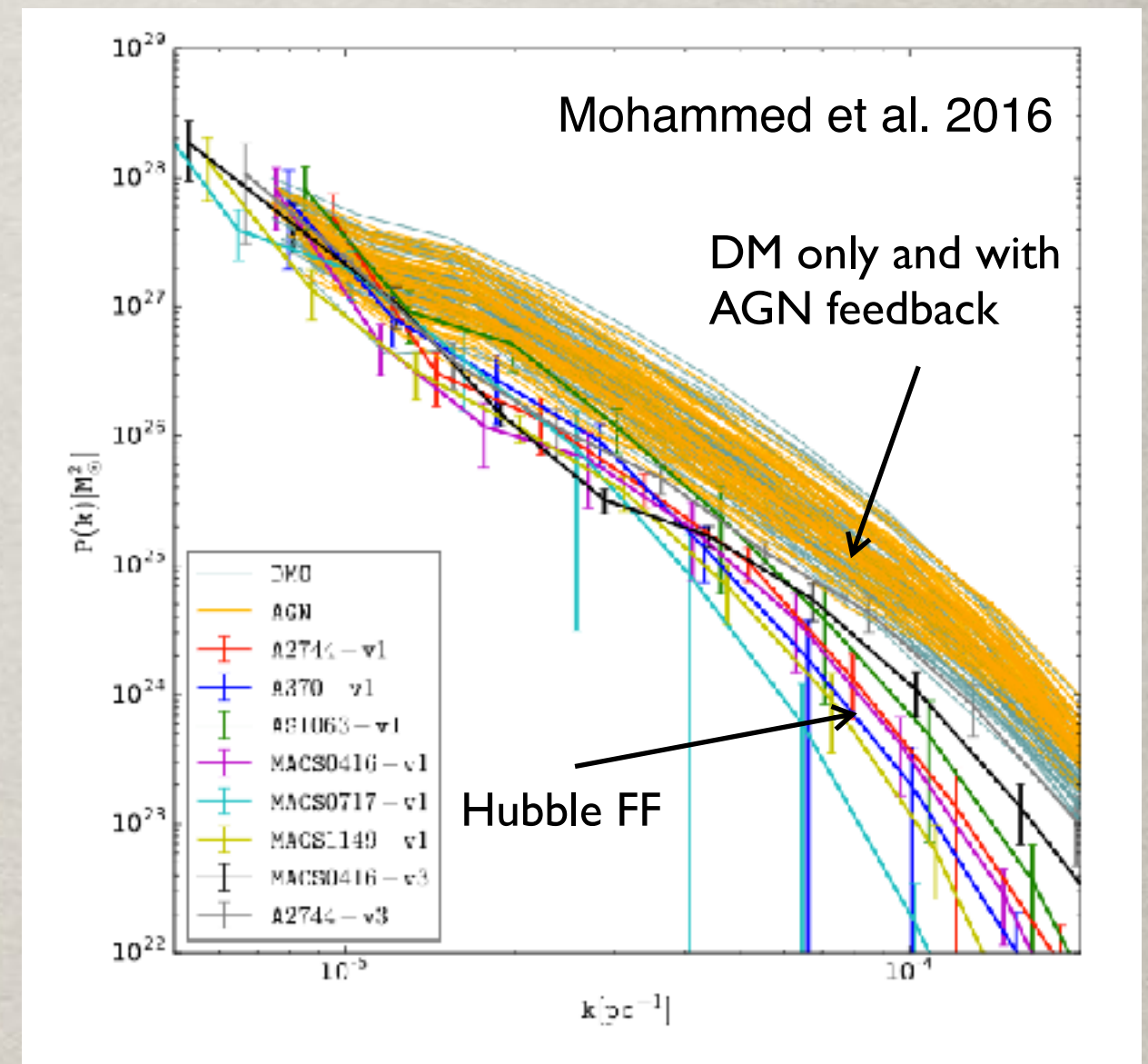
- Quantifying substructures in HFF



Direct detection of substructure in clusters

Sub-halo power spectrum:

- Quantifying substructures in HFF
- Free form modeling: smaller power
- Evidence for WDM (Mohammed et al. 2016)
- Parametric (LTM) finds excess power: upper limit on self-interaction (Jauzac, M., et al., 2016)
- Free form agrees with LTM up to ~ 10 kpc (Sebesta et al. 2016)
[139 lensed images]



Light-Matter Offsets

- Self-Interacting Dark-Matter predicts offsets between luminous and dark matter in dense regions: Smoking gun for SIDM
- Williams and Saha (2011): kpc-scale offsets in Abell 3827 from Free form modeling -> lower limit in cross section
- Mohamed et al. (2014): Abell 3827 and also Abell 2218, no LoS
- Schaller (2015): tension with CDM
- Harvey et al. (2015), 347, 1462; arXiv:1503.07675, upper limit on SIDM
- Kahlhoefer, et al. (2015), Wittman et al. (2017): constraints overestimated
$$\sigma_{DM}/m_{DM} \lesssim 2 \text{ cm}^2/\text{g}$$
- Monteiro-Oliveira, et al. 2017: simulations (CDM + gas + galaxies)
- Interacting systems. Not seen in field galaxies and relaxed clusters

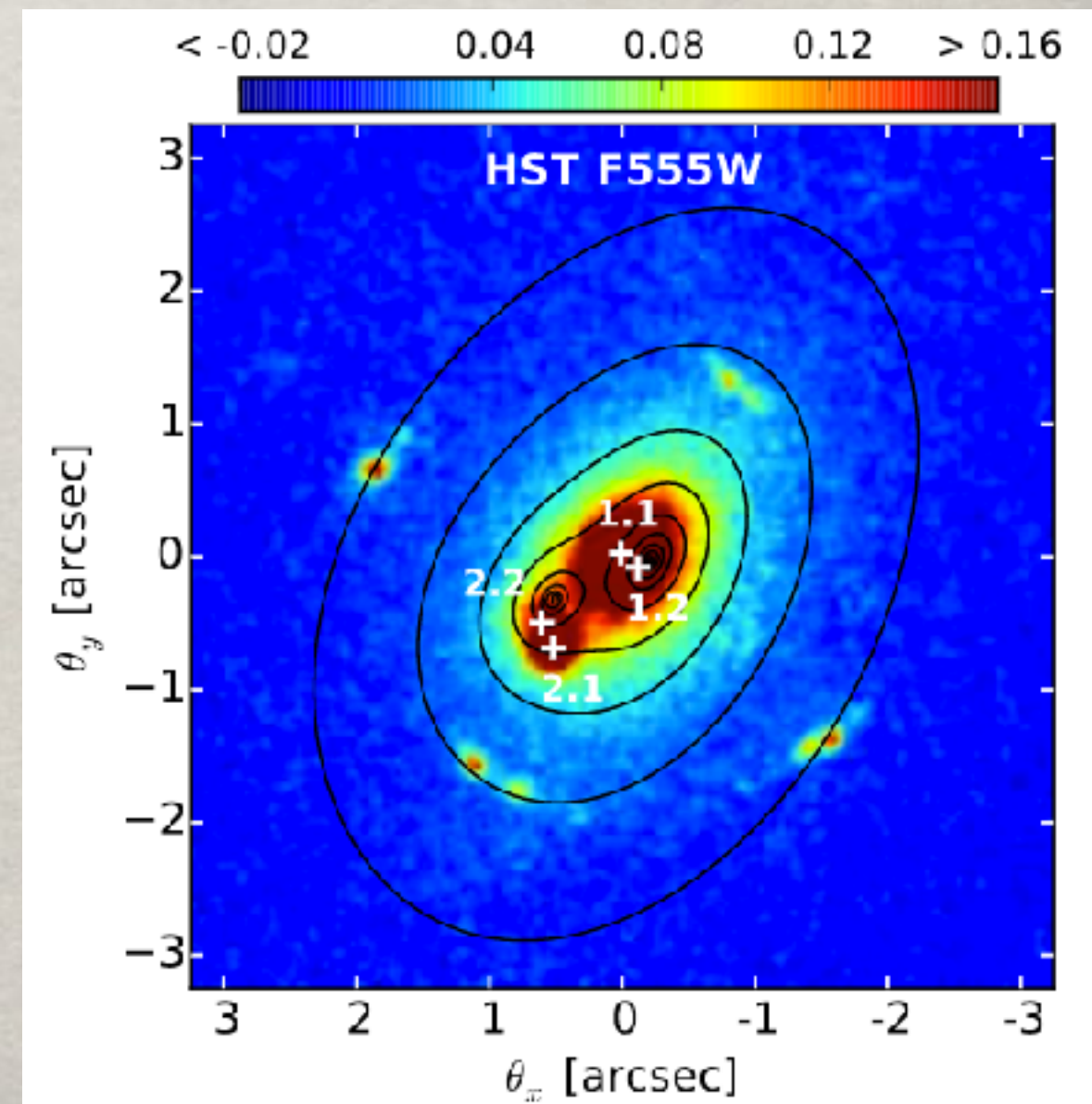
GALAXY SCALE LENSES

- Self-Interacting Dark-Matter predicts offsets between luminous and dark matter in dense regions
 - Seen in clusters, e.g., Harvey et al., 2015, *The nongravitational interactions of dark matter in colliding galaxy clusters*, Science, 347, 1462 (2015); arXiv:1503.07675
- offsets found in a galaxy scale system

- Interacting systems
- kpc offsets in SDSS J1011+0143
(Shu et al. 2015)
- If interpreted solely as evidence for self-interacting dark matter:

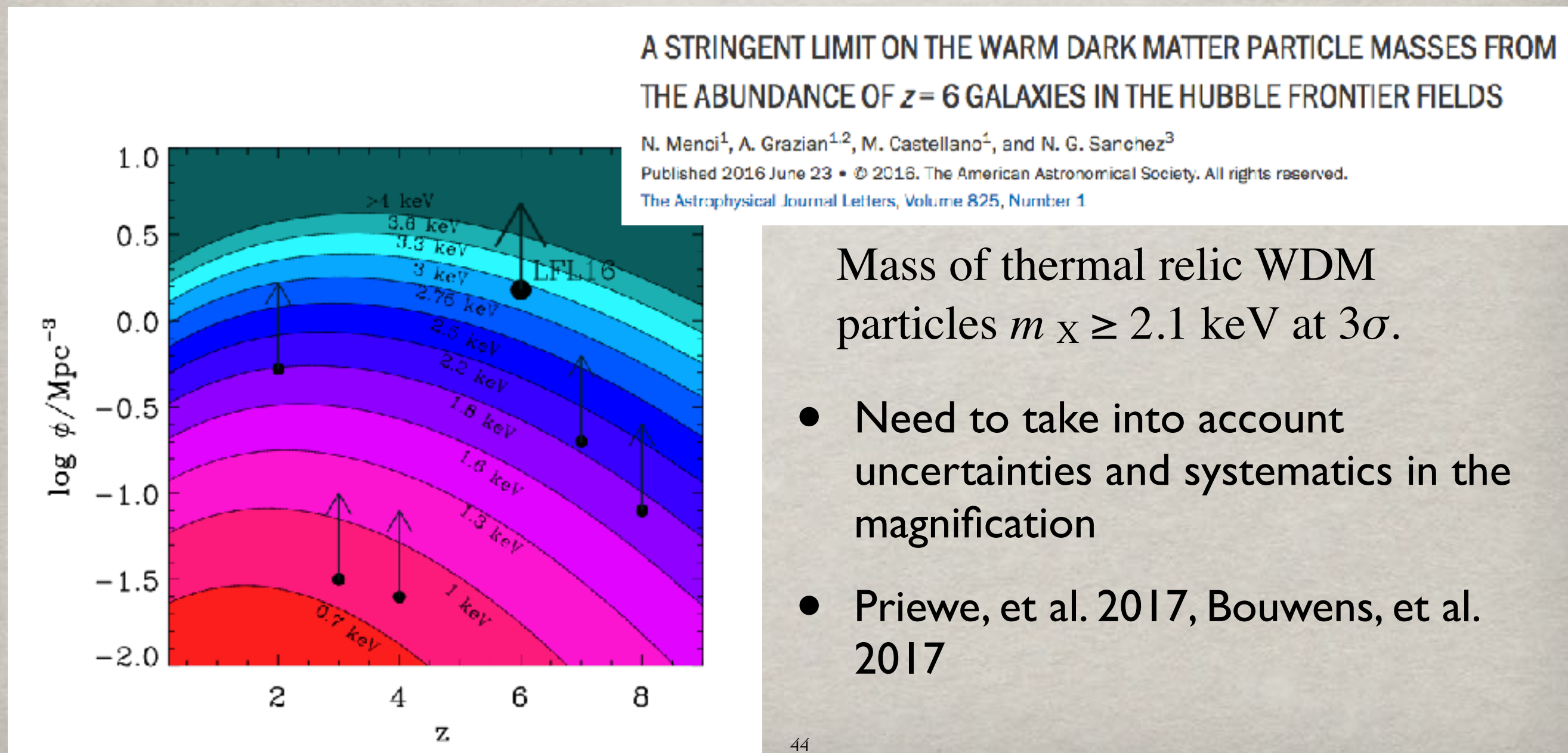
$$\sigma_{\text{DM}}/m \sim (1.7 \pm 0.7) \times 10^{-4} \text{ cm}^2 \text{ g}^{-1} \times (t_{\text{infall}}/10^9 \text{ yr})^{-2}$$

- only SDSS spectroscopy



Gravitational telescopes: luminosity function of ultra-faint UV galaxies at high-redshift

- Warm Dark Matter produces a cutoff in the matter power spectrum (Bode et al. 2001) and thus on the halo mass function



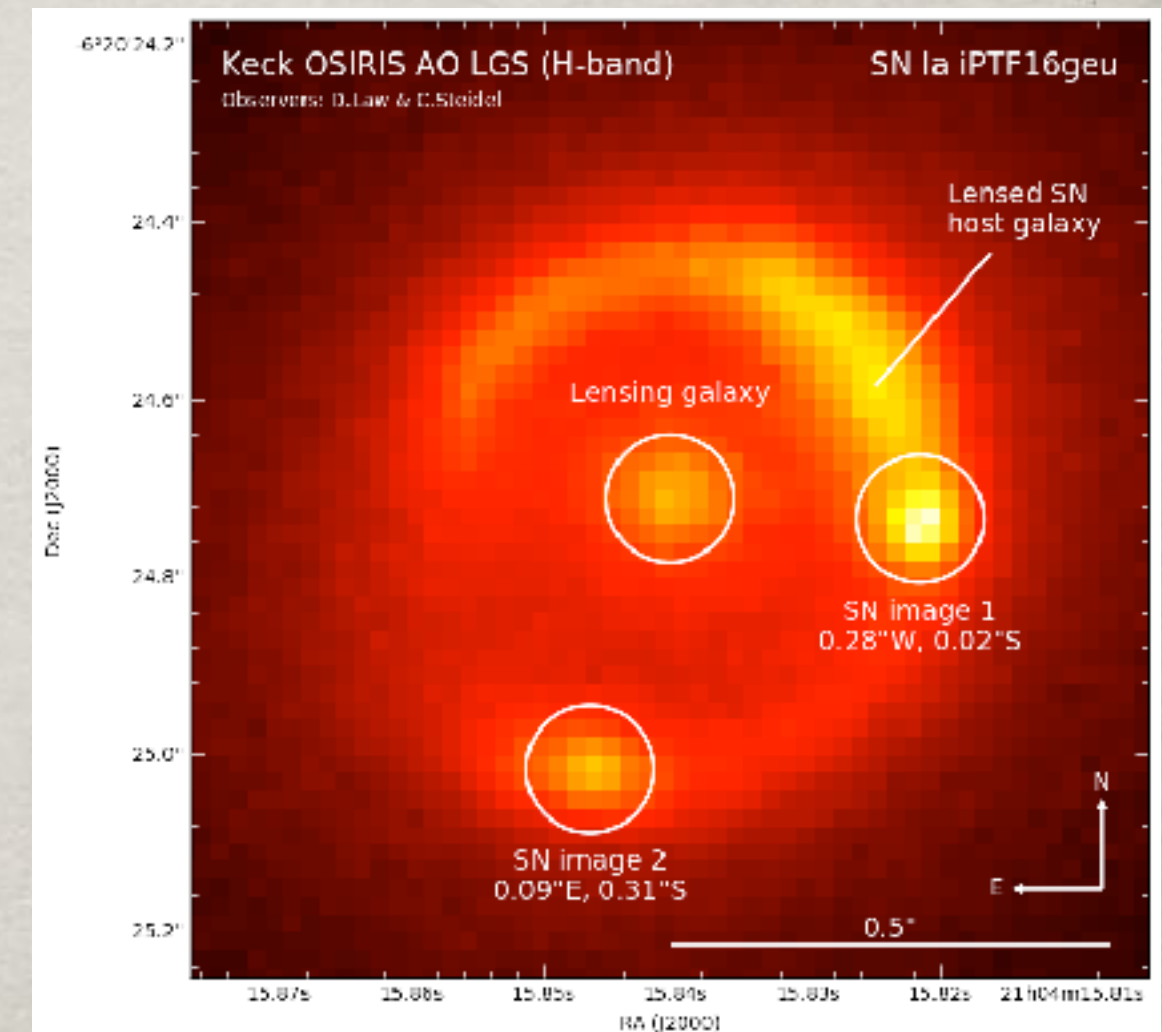
GALAXY SCALE LENSES

- Einstein rings

- Probing mass profiles
- Modified gravity
- HST (SLACS/BOSS), CFHTLS

- Time delays

- H_0 , time delay distance
- Angular diameter distance
- HST mass models
- Supernovae!

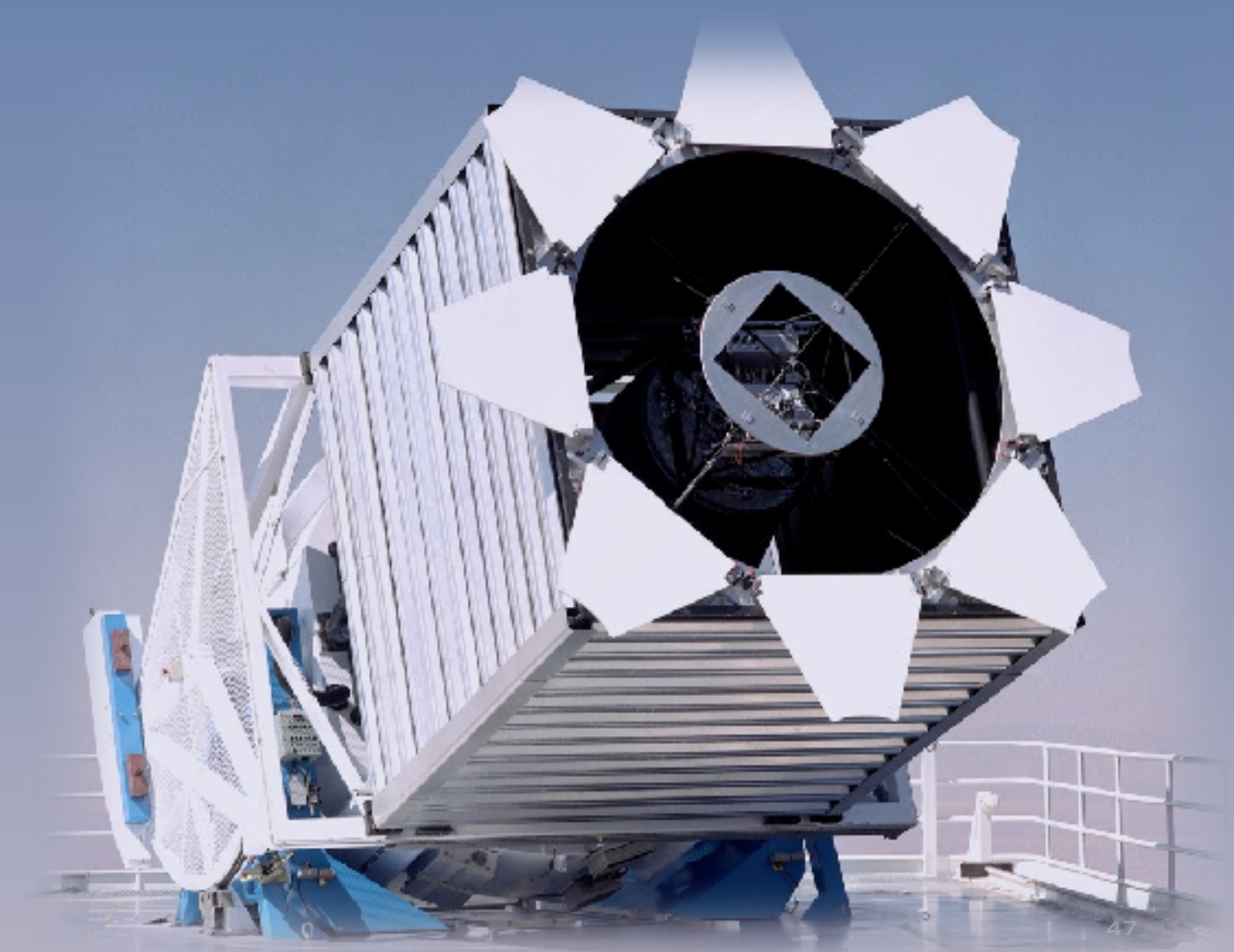


Goobar et al., The discovery of the multiply-imaged lensed Type Ia supernova iPTF16geu, arXiv:1611.00014

¿COMO ENCONTRAR LENTES FUERTES?

BUSCA EM ESPECTROSCOPIA: EXEMPLO DO SDSS

E BOSS



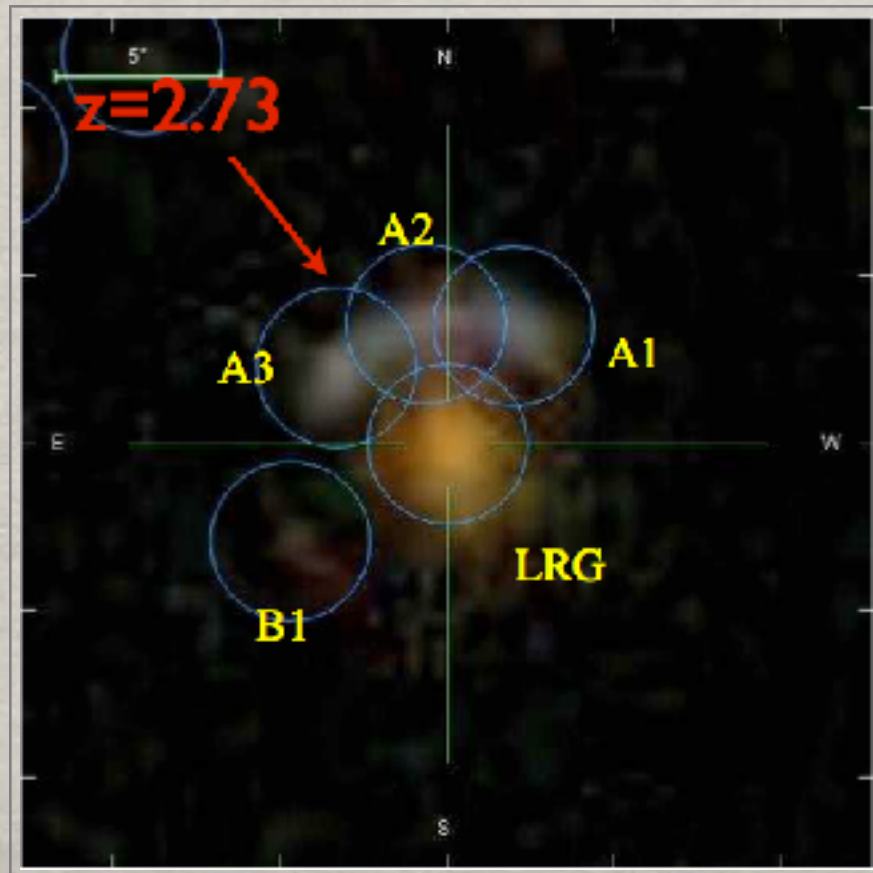


SDSS III

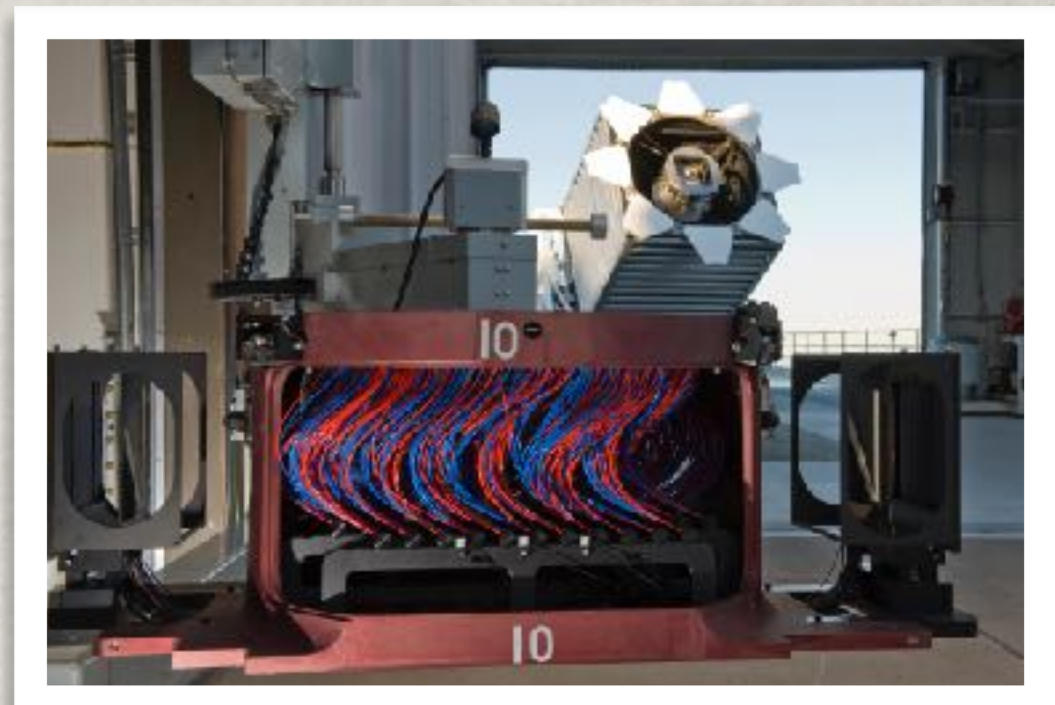
BOSS

Imagens:

- Fotometria completada: $\sim 10.000 \text{ deg}^2$ ($> \frac{1}{4}$ do céu)
- Espectroscopia
- 1000 espectros por exposição
- 1.5 milhões de z



SDSS III
BRAZILIAN PARTICIPATION GROUP



Foco principal: OAB

Inclusão da direção radial: H_0

Também aglomerados e lentes:

proposta auxiliar: BCGs na faixa 82

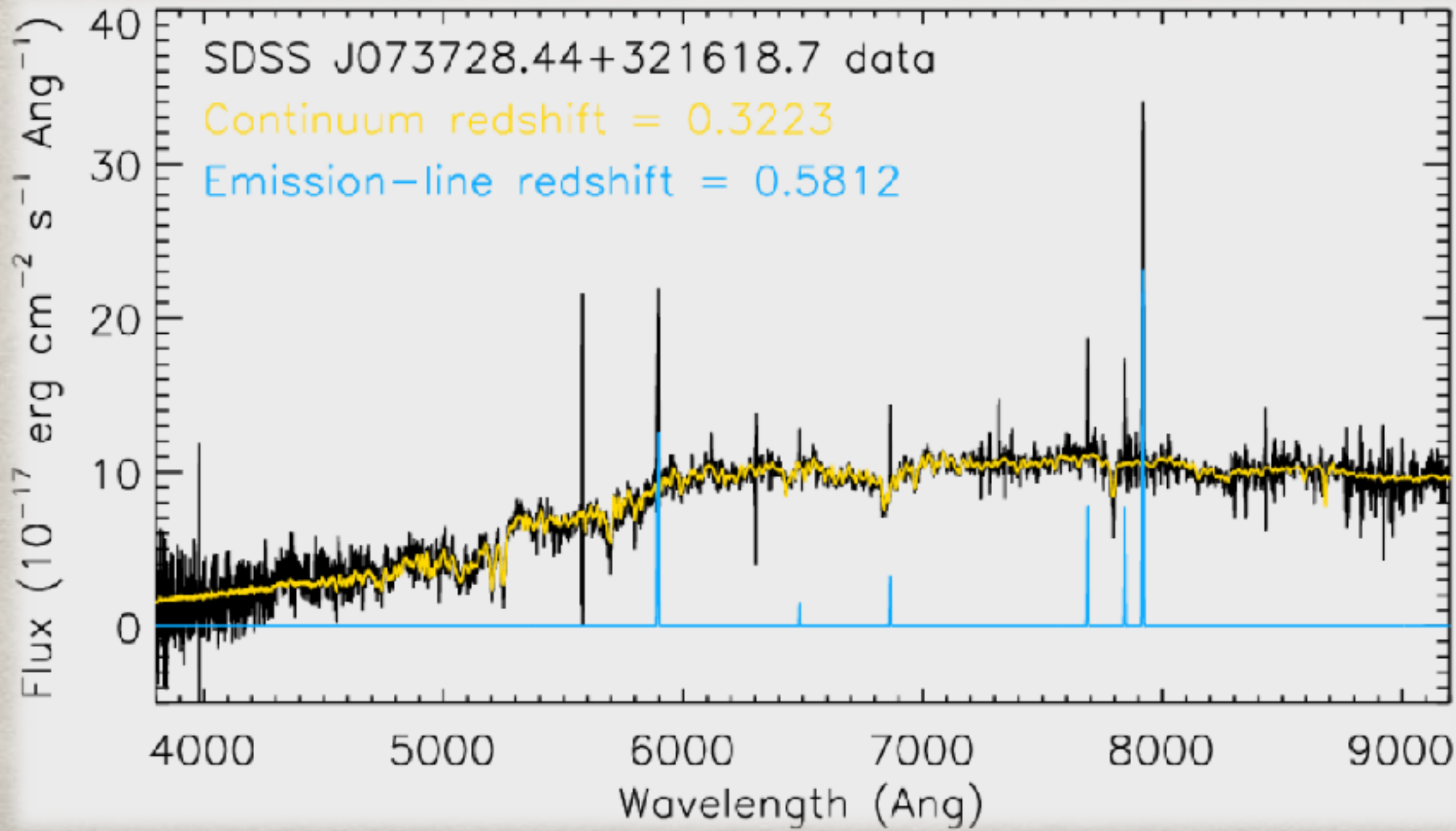
Lensing Working Group

Galaxy Evolution Working Group

BELLS: BOSS EMISSION-LINE LENS SURVEY

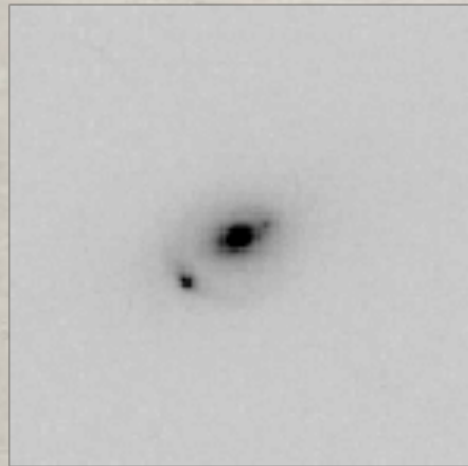
- Continuação do SLACS

ONE SPECTRUM, TWO REDSHIFTS

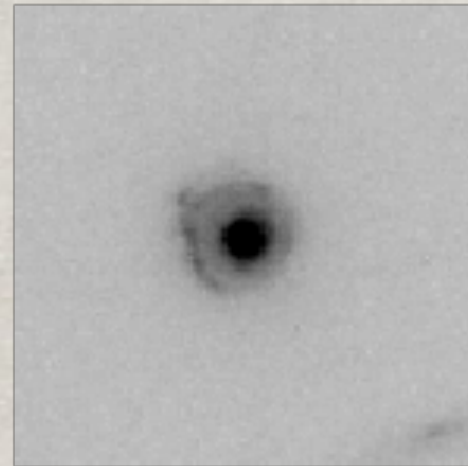


Bolton, 2010

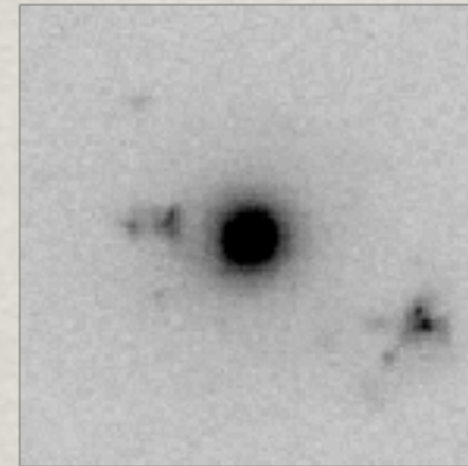
IMAGENS COM O HST



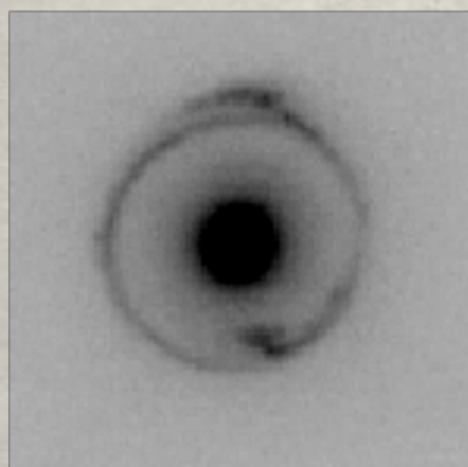
(a) SDSS J0151+0049
 $z_1 = 0.517103, z_2 = 1.36357$



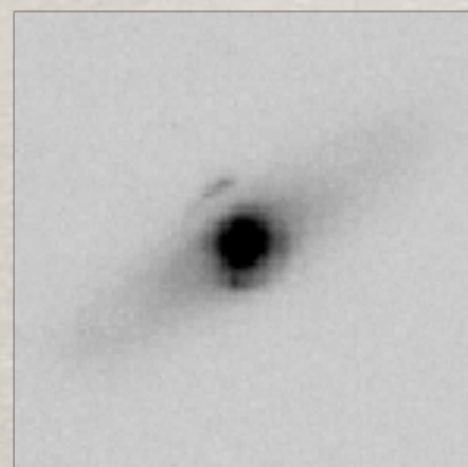
(b) SDSS J0801+4727
 $z_1 = 0.483035, z_2 = 1.51807$



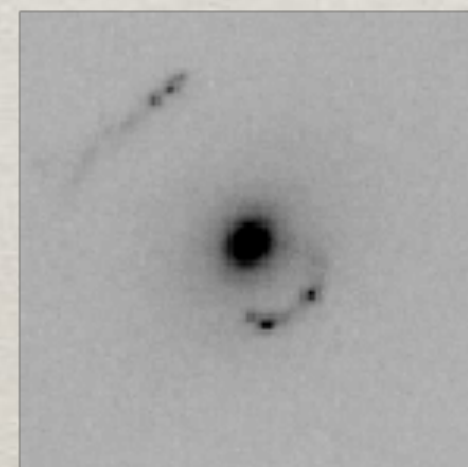
(c) SDSS J1352+3216
 $z_1 = 0.463428, z_2 = 1.03361$



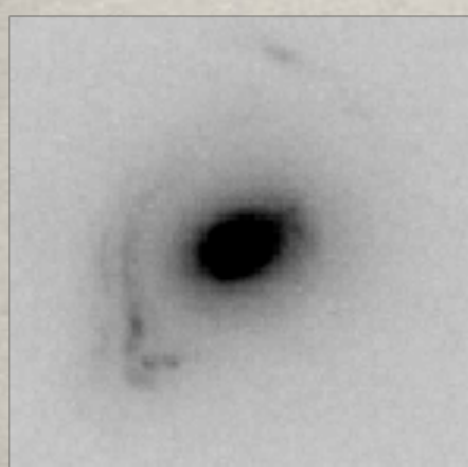
(d) SDSS J1631+1854
 $z_1 = 0.40797, z_2 = 1.08626$



(e) SDSS J1637+1439
 $z_1 = 0.390852, z_2 = 0.874424$



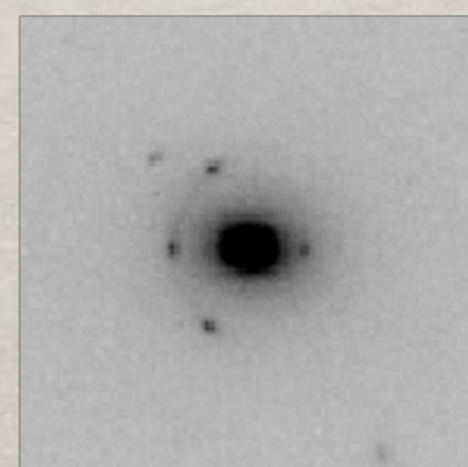
(f) SDSS J2122+0409
 $z_1 = 0.626099, z_2 = 1.4517$



(g) SDSS J2125+0411
 $z_1 = 0.36318, z_2 = 0.977278$



(h) SDSS J1541+1812
 $z_1 = 0.560163, z_2 = 1.11333$



(i) SDSS J2303+0037
 $z_1 = 0.458262, z_2 = 50.936278$

Bolton et al., 2010

□ 45 alvos com o HST Cycle 18 (1 órbita em F814W cada)

□ Taxa de sucesso

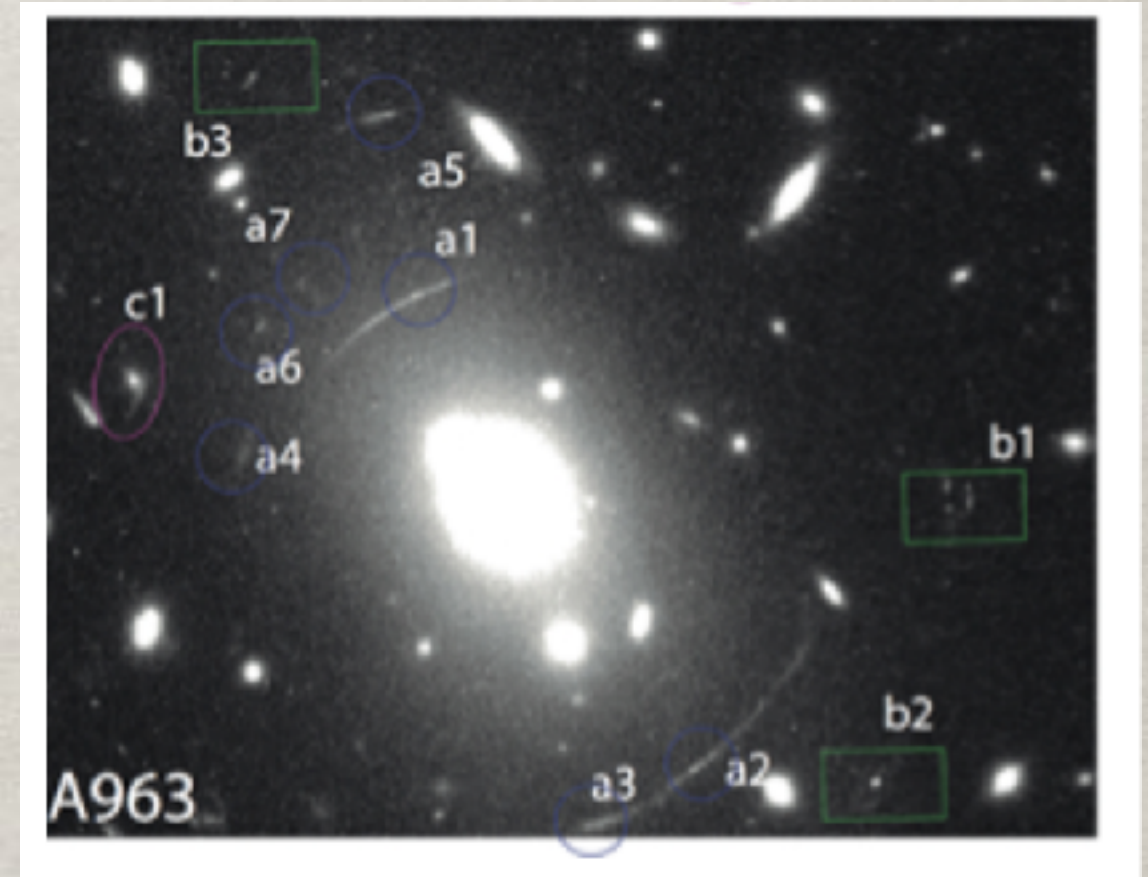
28 observados

~14 lentes confirmadas

recortes de 7.5" x 7.5"

BÚSQUEDA EN IMÁGENES

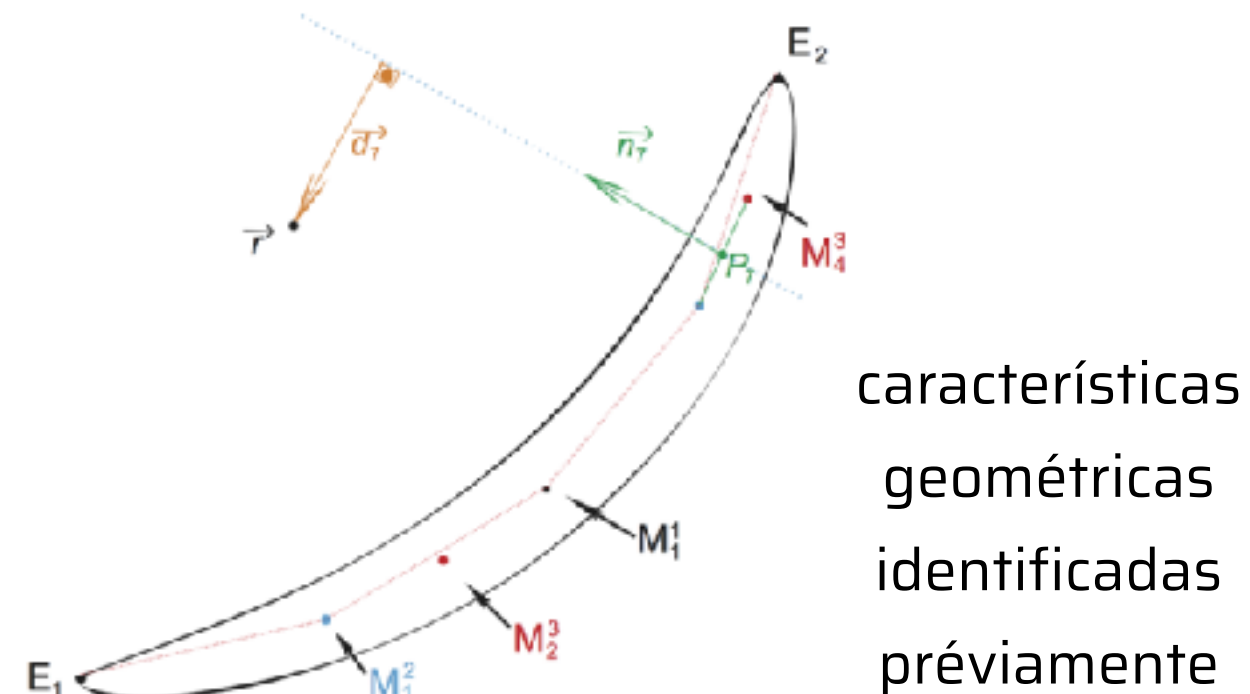
- ✿ ¡Hay un sistema con arcos a cada ~ 100.000 galaxias!
- ✿ Busca automática
- ✿ 2010-2017: red neuronal completamente conectada, máximo 9 características, 1 capa interna!!
(max 16 neuronas)
[~ 500 objetos]



A neural network gravitational arc finder based on the Mediatrix filamentation method

C. R. Bom^{1,2}, M. Makler¹, M. P. Albuquerque¹, and C. H. Brandt^{3,4,5}

- Conjunto etiquetado: 175 (!) arcos gravitacionales simulados + 437 no arcos
- Entrenamiento 80%, validación 20%
- Métricas
 - True positive rate (TPR)
 - False positive rate (FPR)



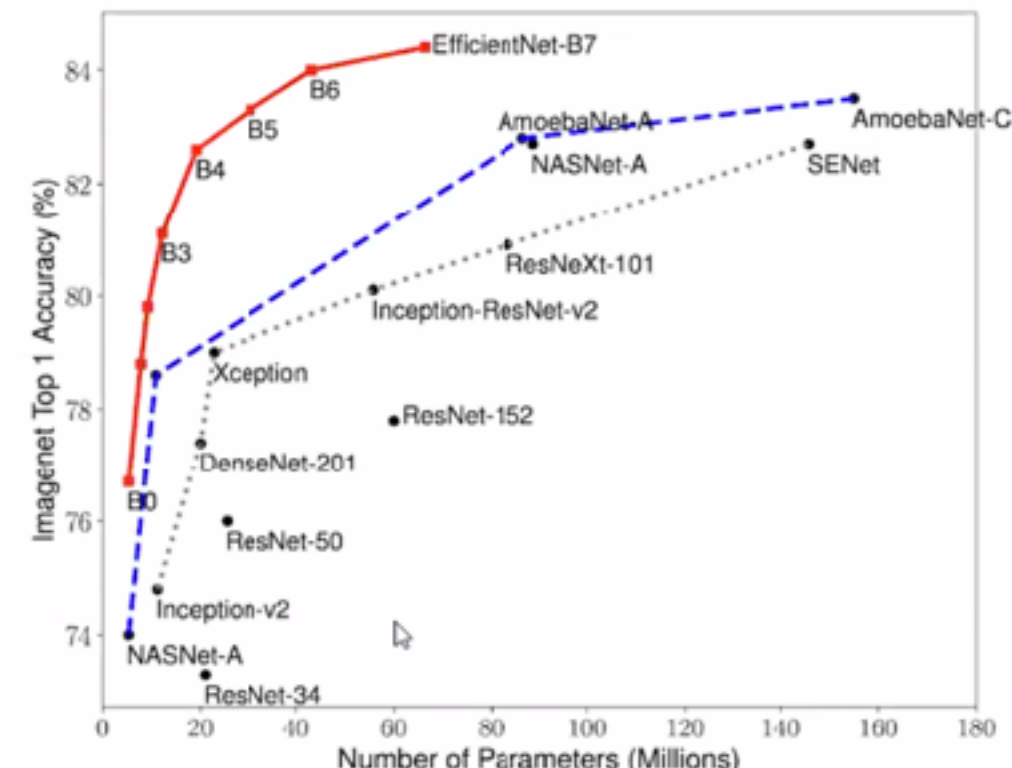
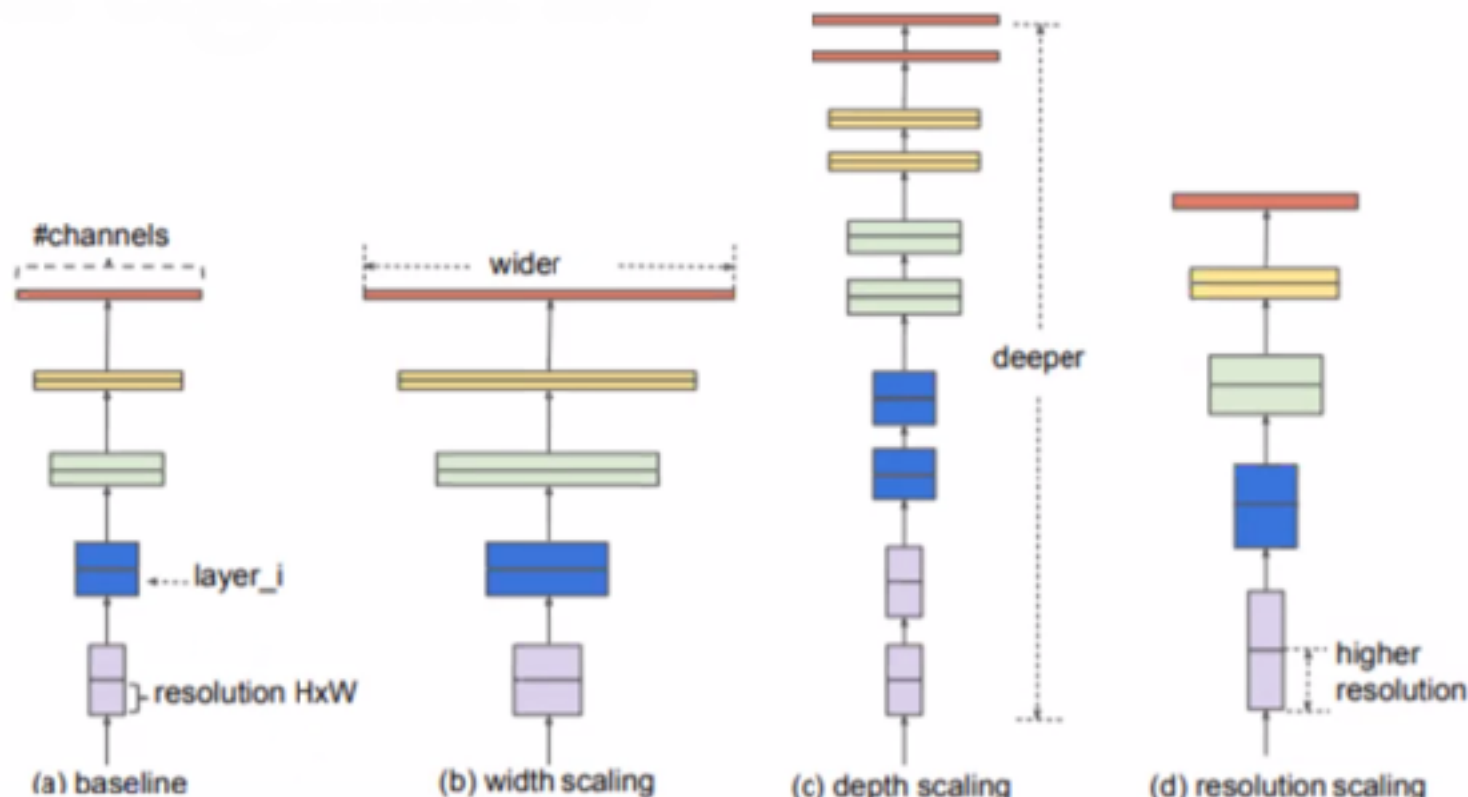
Y LLEGÓ EL DEEP LEARNING...

- ✿ Buscar arcos gravitacionales (resultantes de la deformación del espacio-tiempo) en imágenes astronómicas
- ✿ 2010-2017: red neuronal completamente conectada, máximo 9 características, 1 capa interna!! (max 16 neuronas)[~ 500 objetos]
- ✿ 2017-2019:
 - ✿ The strong gravitational lens finding challenge, 20 000 imágenes, 4 canales, 101 x 101 pixeles
 - ✿ CNN con 20 filtros de 5×5 (+SVN)
 - ✿ Tercer lugar (arXiv:1802.03609)
- ✿ 2022: The strong gravitational lens finding challenge II
 - ✿ 100 000 imágenes [4 canales]
 - ✿ Pruebas con varias arquitecturas y configuraciones. Modelo final: EfficientNet
 - ✿ ¡GPUs trabajando en conjunto!
 - ✿ Primer lugar!!

EfficientNet Model

Based on compound scaling method is to perform a grid search to find a baseline model, named B0.

depth: $d = \alpha^\phi$
width: $w = \beta^\phi$
resolution: $r = \gamma^\phi$



Later, it optimizes the relationship between different scaling dimensions of the baseline network under a FLOPS constraint.

Automatización de la búsqueda y del modelado de los sistemas

Hay ~ 1 anillo de Einstein a cada $O(100.000)$ galáxias
Surveys futuros: $O(10.000.000.000)$ de galaxias!

Gravitational Lens Finding Challenge 2

- Simulaciones de sistemas según lo que se espera para la sonda espacial Euclid
- Usamos métodos de Deep Learning para identificar y **medir** los sistemas

Challenge 2.0

Update Feb. 28, 2020 We have a winner!! C. Bom, et al.'s "Cast_efficient_auc" entry has won. Congratulations to them and everyone else. There were several very close entries. Detailed report to follow...

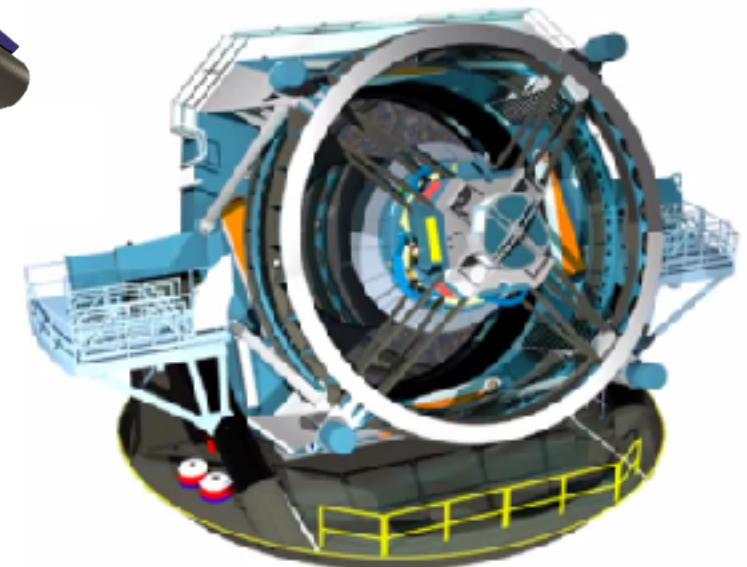
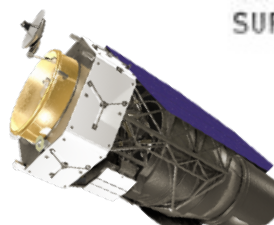
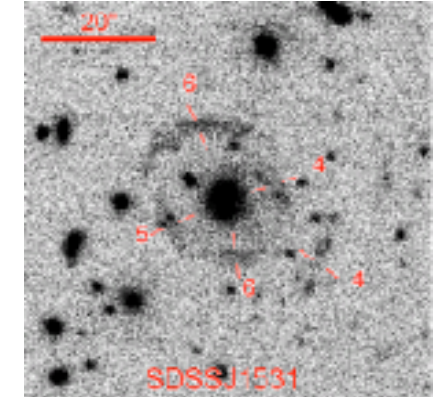
Challenge 2.0 is an improvement in the simulated images over 1.0 and a change in the bands. This challenge concentrates only on Euclid-like observations in the VIS, and NISP J, Y and H bands. The pixels sizes are 0.1" for VIS and 0.3" for J, Y and H. The training and the test sets consists of 100,000 images in each band.

This project is funded by the European Union's Horizon 2020 research and innovation programme under grant agreement No. 259341. 

Past, present and future

Homogeneous Strong Lensing Samples (arcs)

- ▶ 1986-2016: $\mathcal{O}(10^2)$ systems
 - ▶ $\mathcal{O}(10^2)$ deg² surveys: CFHTLS/SL2S, SOGRAS, CS82
 - ▶ Spectroscopy + HST: SLACS, BELLS
- ▶ 2016-2024: $\mathcal{O}(10^3)$ systems
 - ▶ $\mathcal{O}(10^3)$ deg² surveys: KiDS, RCSLens, DES, HSC, DELVE
 - ▶ Spectroscopy: SDSS/SILO, SWELLS, SL4TM
 - ▶ automated arcfinding
- ▶ > 2024: $\mathcal{O}(10^4 - 10^5)$ systems
 - ▶ Rubin/LSST, EUCLID, Roman/WFIRST
 - ▶ Rubin: ~ 100 strongly lensed supernovae!
 - ▶ DESI, Subaru PFS/SUMIRE, 4MOST



LSST: 1/2 sky per night, 10^{10} galaxies! (+DDF+TD)

- ▶ arcfinding codes
- ▶ automated analyses (ML, everywhere, lots to do)

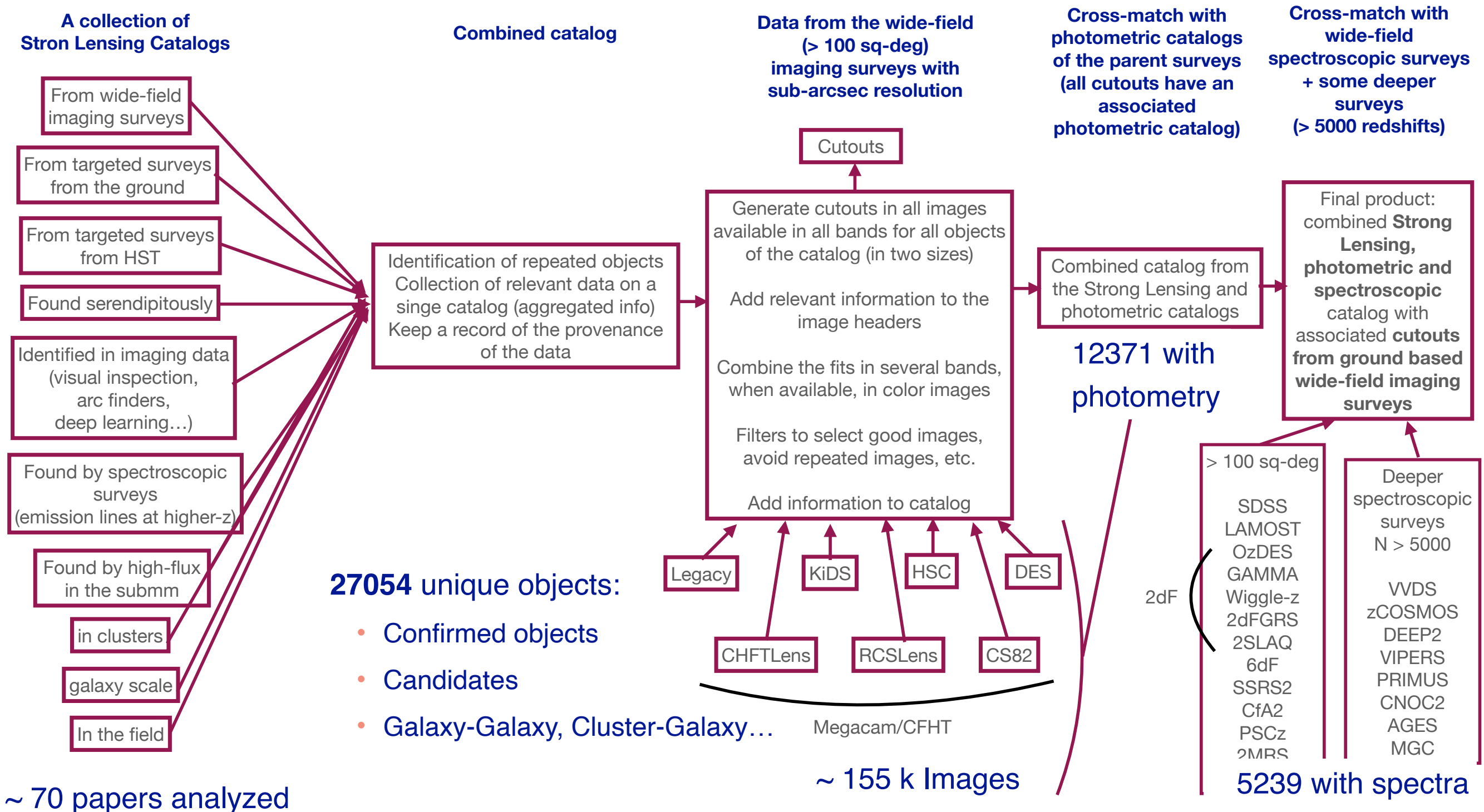
Telescopio Vera Rubin y su LSST

Estado del arte de la astronomía por imágenes con *seeing* natural

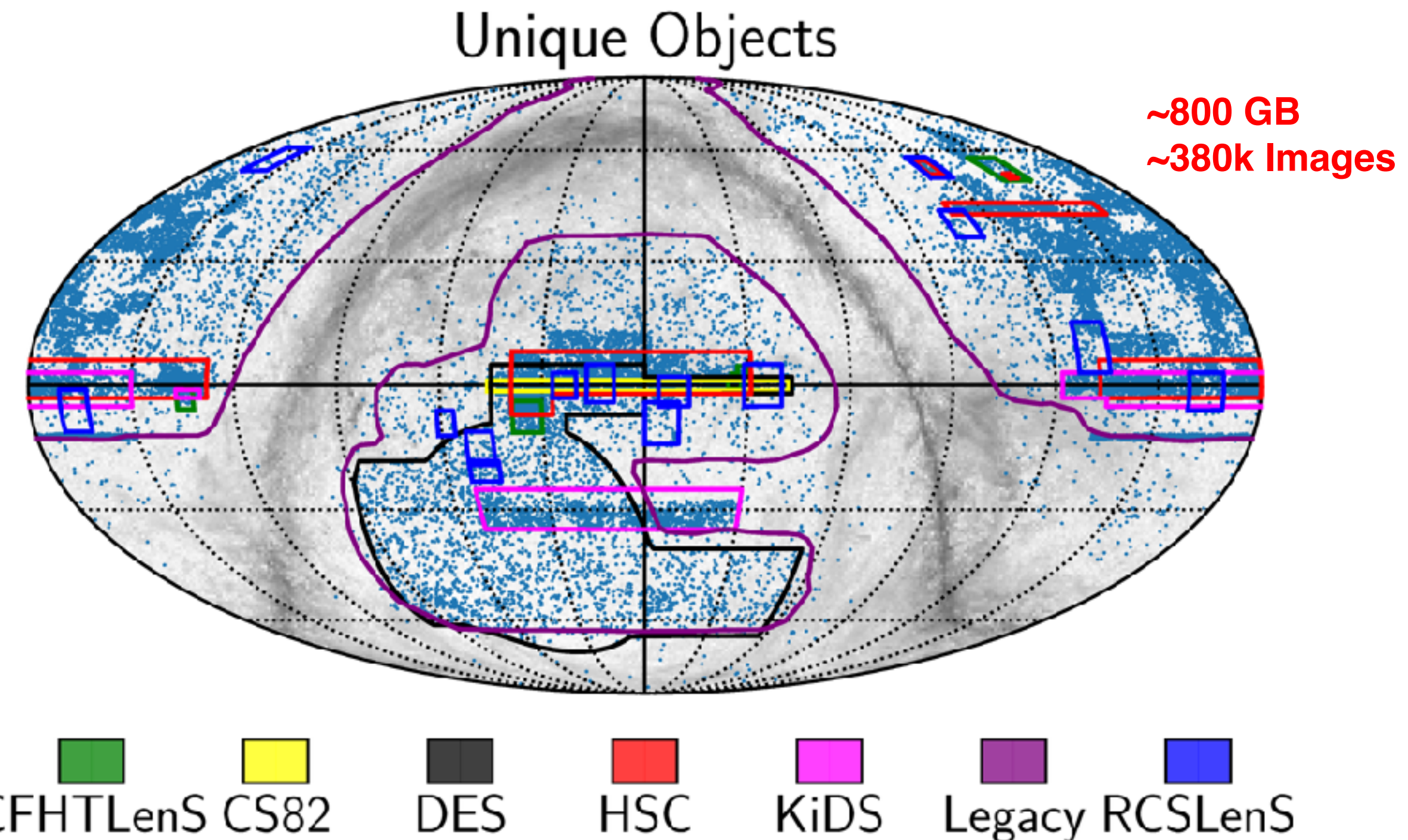
- Observatorio completamente nuevo en Cerro Pachón, Chile (con Gemini y SOAR)
- Gran apertura, luminosidad y campo de visión: espejo primario de 8.4 m, nuevo diseño óptico $f/1.2$
- Cámara de 10 sq-deg en 3.2 Gpx (mayor cámara del mundo)
- **CCDs gruesas (sensible al rojo) y de lectura rápida (2s!)**
- Habilidad de exposiciones cortas, totalmente automatizado
- Instrumento **ideal y único para relevamientos**
- **No solo el próximo paso: nueva dimensión temporal!**
- 1 millón de alertas por noche!
- Inicio del *survey* con la cámara completa: 2024
- Contribución *in-kind* del IATE/AOC/UNC: membresía en LSST!



The last stand before LSST: A collection of Strong Lensing Systems with Ground Based Images from Wide-Field Surveys

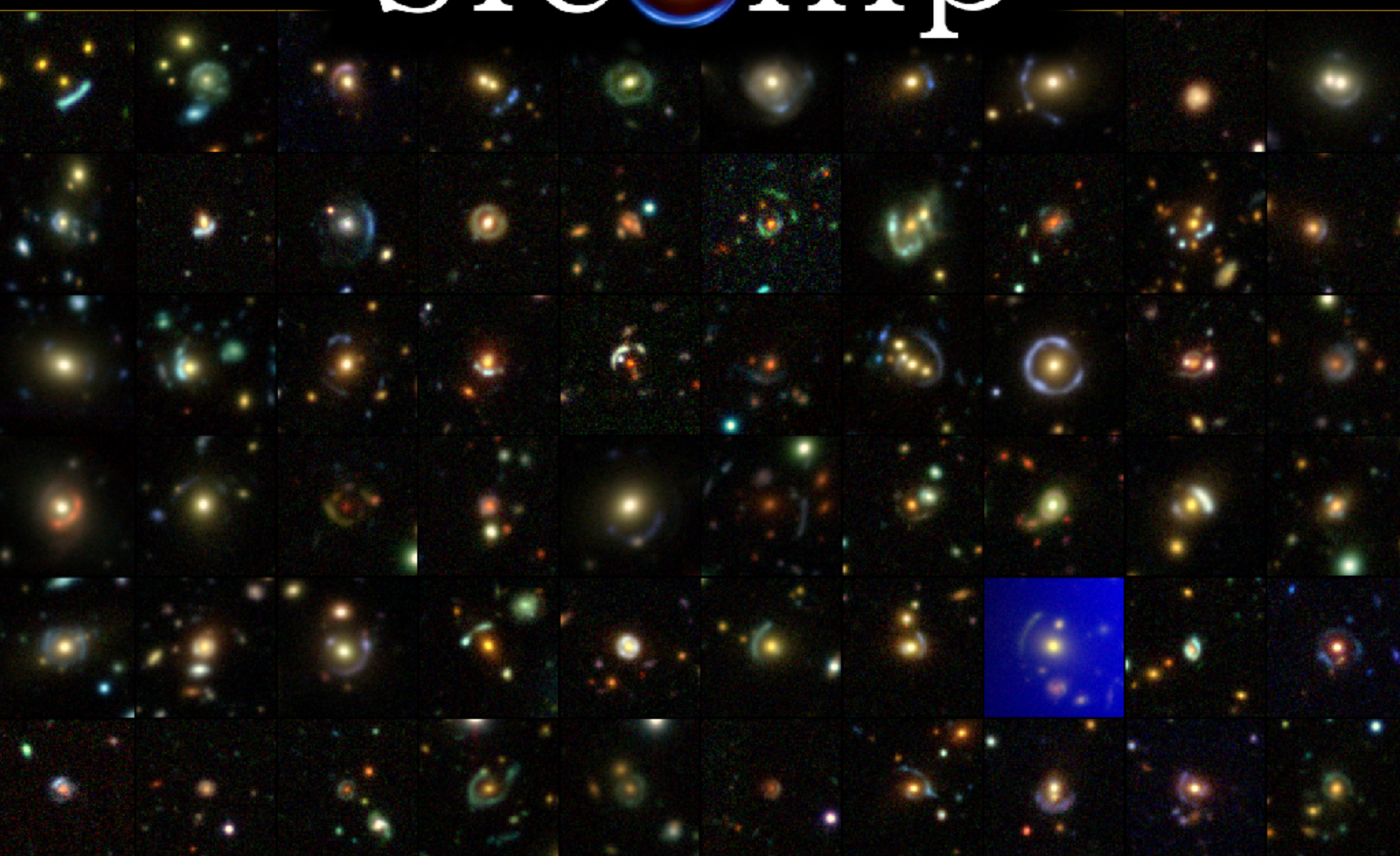


The last stand before LSST: A collection of Strong Lensing Systems with Ground Based Images from Wide-Field Surveys



slcomp

Some systems....





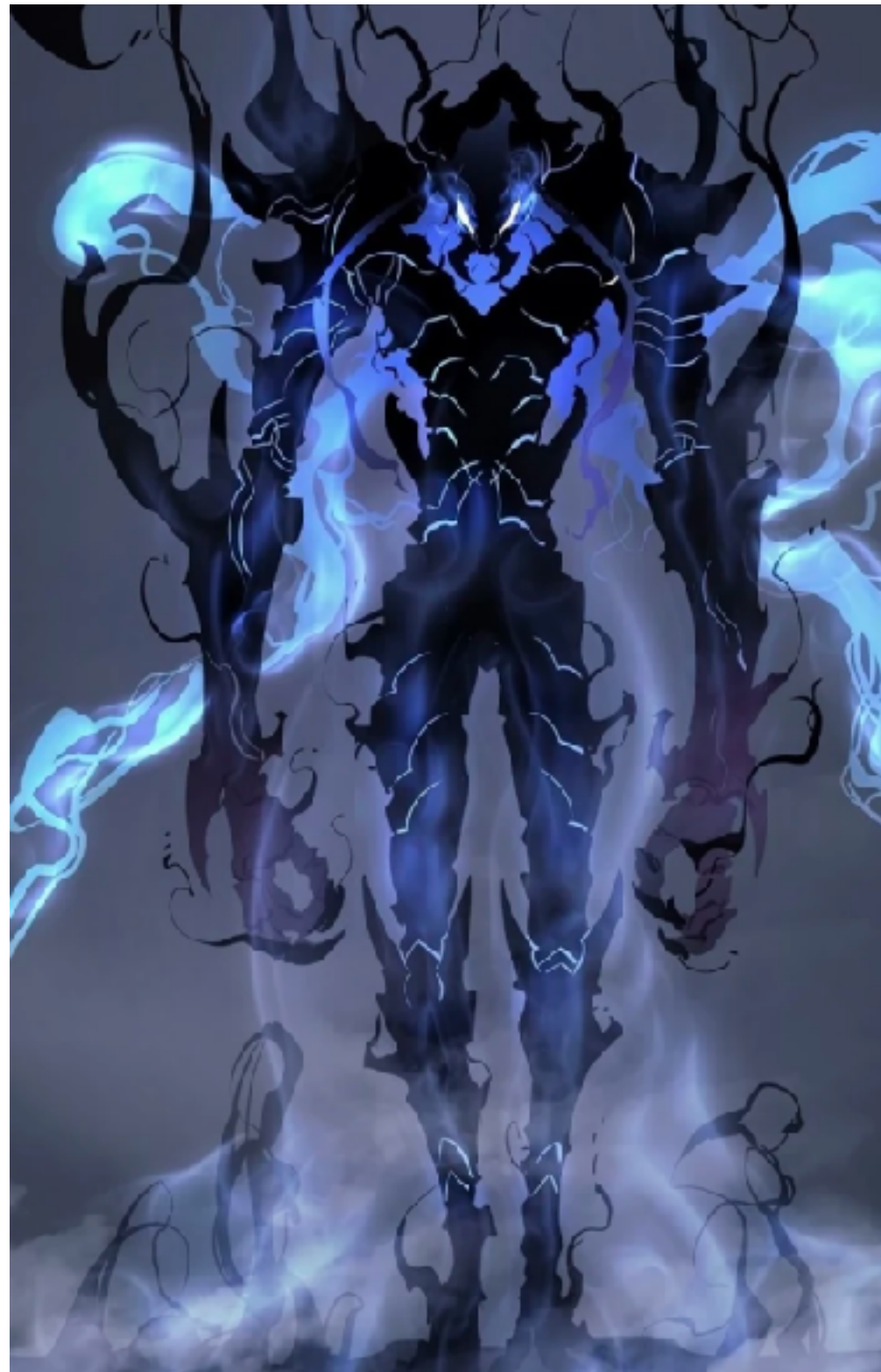
- slcomp: a semi-automated infrastructure for the aggregation of SL systems, cross matches, and generation of cut-outs
- current version: **Last Stand Before Rubin**

LaStBeRu

- ongoing work:
 - visual inspection: vetting + tagging (zooniverse, ML applications - SLImageNet)
 - massive modelling + time delay predictions (new)

베루

LaStBeRu



Groovy, cool, or otherwise something good or favored



¡El fin de la división entre microlensing y strong lensing!

First Resolution of Microlensed Images of a Binary-Lens Event

ZEXUAN WU ,^{1, 2} SUBO DONG ,^{1, 2, 3} A. MÉRAND ,⁴ CHRISTOPHER S. KOCHANEK,^{5, 6}
PRZEMEK MRÓZ ,⁷ JINYI SHANGGUAN,⁸ GRANT CHRISTIE,⁹ THIAM-GUAN TAN ,¹⁰
THOMAS BENSBY ,¹¹ JOSS BLAND-HAWTHORN ,^{12, 13} SVEN BUDER ,^{14, 13} FRANK EISENHAUER,^{8, 15}
ANDREW P. GOULD,^{16, 5} JANEZ KOS ,¹⁷ TIM NATUSCH,^{18, 9} SANJIB SHARMA ,^{12, 13}
ANDRZEJ UDALSKI ,⁷ J. WOILLEZ,⁴ DAVID A. H. BUCKLEY¹⁹ AND I. B. THOMPSON²⁰

KARIM ABD EL DAYEM,²¹ EVELYNE ALECIAN,²² CARINE BABUSIAUX,²² ANTHONY BERDEU,²¹
JEAN-PHILIPPE BERGER,²² GUILLAUME BOURDAROT,⁸ WOLFGANG BRANDNER,¹⁶ MAICA CLAVEL,²²
RICHARD I. DAVIES,⁸ DENIS DEFREÈRE,²³ CATHERINE DOUGADOS,²² ANTONIA DRESCHER,⁸
ANDREAS ECKART,^{24, 25} MAXIMILIAN FABRICIUS,⁸ HELMUT FEUCHTGRUBER,⁸
NATASCHA M. FÖRSTER SCHREIBER,⁸ PAULO GARCIA,^{26, 27} REINHARD GENZEL,^{8, 28}
STEFAN GILLESSEN,⁸ GERNOT HEİBEL,²¹ SEBASTIAN HÖNIG,²⁹ MATHIS HOULLE,³⁰
PIERRE KERVELLA,²¹ LAURA KREIDBERG,¹⁶ SYLVESTRE LACOUR,^{21, 4} OLIVIER LAI,³⁰
ROMAIN LAUGIER,²³ JEAN-BAPTISTE LE BOUQUIN,²² JAMES LEFTLEY,³⁰ BRUNO LOPEZ,³⁰
DIETER LUTZ,⁸ FELIX MANG,⁸ FLORENTIN MILLOUR,³⁰ MIGUEL MONTARGÈS,²¹ HUGO NOWACKI,²²
MATHIAS NOWAK,²¹ THOMAS OTT,⁸ THIBAUT PAUMARD,²¹ KARINE PERRAUT,²² GUY PERRIN,²¹
ROMAIN PETROV,³⁰ PIERRE-OLIVIER PETRUCCI,²² NICOLAS POURRE,²² SEBASTIAN RABIEN,⁸
DIOGO C. RIBEIRO,⁸ SYLVIE ROBBE-DUBOIS,³⁰ MATTEO SADUN BORDONI,⁸ DARYL SANTOS,⁸
JONAS SAUTER,¹⁶ JULES SCIGLIUTO,³⁰ TARO T. SHIMIZU,⁸ CHRISTIAN STRAUBMEIER,²⁴
ECKHARD STURM,⁸ MATTHIAS SUBROWEIT,²⁴ CALVIN SYKES,²⁹ LINDA TACCONI,⁸
FRÉDÉRIC VINCENT²¹ AND FELIX WIDMANN⁸